fragments act in concert to cause mitochondrial dysfunction and neurotoxicity. *Proceedings of the National Academy of Sciences* 2005, **102**:18694-18699.

30. Mahley RW, Hui DY, Innerarity TL, Beisiegel U: **Chylomicron remnant metabolism. Role of hepatic lipoprotein receptors in mediating uptake.** *Arteriosclerosis* 1989, **9**:114-8.
31. Tanaka M, Vedhachalam C, Sakamoto T, Dhanasekaran P, Phillips MC, Lund-Katz S, Saito H: **Effect of carboxyl-terminal truncation on structure and lipid interaction of human apolipoprotein E4.** *Biochemistry* 2006, **45**:4240-7.
32. Pillot T, Goethals M, Najib J, Labeur C, Lins L, Chambaz J, Brasseur R, Vandekerckhove J, Rosseneu M: **Beta-amyloid peptide interacts specifically with the carboxy-terminal domain of human apolipoprotein E: relevance to Alzheimer's disease.** *J Neurochem* 1999, **72**:230-7.
33. Phu MJ, Hawbecker SK, Narayanaswami V: **Fluorescence resonance energy transfer analysis of apolipoprotein E C-terminal domain and amyloid beta peptide (1–42) interaction.** *J Neurosci Res* 2005, **80**:877-86.
34. Caspersen C, Wang N, Yao J, Sosunov A, Chen X, Lustbader JW, Xu HW, Stern D, McKhann G, Yan SD: **Mitochondrial Abeta: a potential focal point for neuronal metabolic dysfunction in Alzheimer's disease.** *Faseb J* 2005, **19**:2040-1.
35. Takahashi RH, Milner TA, Li F, Nam EE, Edgar MA, Yamaguchi H, Beal MF, Xu H, Greengard P, Gouras GK: **Intraneuronal Alzheimer abeta42 accumulates in multivesicular bodies and is associated with synaptic pathology.** *Am J Pathol* 2002, **161**:1869-79.
36. Martin BL, Schrader-Fischer G, Busciglio J, Duke M, Paganetti P, Yankner BA: **Intracellular Accumulation of beta-Amyloid in Cells Expressing the Swedish Mutant Amyloid Precursor Protein.** *J Biol Chem* 1995, **270**:26727-26730.
37. Chui DH, Tanahashi H, Ozawa K, Ikeda S, Checler F, Ueda O, Suzuki H, Araki W, Inoue H, Shirotani K, Takahashi K, Gallyas F, Tabira T: **Transgenic mice with Alzheimer presenilin 1 mutations show accelerated neurodegeneration without amyloid plaque formation.** *Nat Med* 1999, **5**:560-4.
38. Wilson CA, Doms RW, Lee VM: **Intracellular APP processing and A beta production in Alzheimer disease.** *J Neuropathol Exp Neurol* 1999, **58**:787-94.
39. Hartmann T: **Intracellular biology of Alzheimer's disease amyloid beta peptide.** *Eur Arch Psychiatry Clin Neurosci* 1999, **249**:291-8.
40. Lovestone S, Anderton BH, Hartley C, Jensen TG, Jorgensen AL: **The intracellular fate of apolipoprotein E is tau dependent and apoe allele-specific.** *Neuroreport* 1996, **7**:1005-8.
41. Hamilton RL, Wong JS, Guo LS, Krisans S, Havel RJ: **Apolipoprotein E localization in rat hepatocytes by immunogold labeling of cryothin sections.** *J Lipid Res* 1990, **31**:1589-603.
42. DeMattos RB, Thorngate FE, Williams DL: **A test of the cytosolic apolipoprotein E hypothesis fails to detect the escape of apolipoprotein E from the endocytic pathway into the cytosol and shows that direct expression of apolipoprotein E in the cytosol is cytotoxic.** *J Neurosci* 1999, **19**:2464-73.

the FEBS Journal

An E3 ubiquitin ligase, Synoviolin, is involved in the degradation of immature nicastrin, and regulates the production of amyloid β-protein

Tomoji Maeda[1], Toshihiro Marutani[2,*], Kun Zou[1], Wataru Araki[3], Chiaki Tanabe[1], Naoko Yagishita[4], Yoshihisa Yamano[4], Tetsuya Amano[4], Makoto Michikawa[2], Toshihiro Nakajima[4,5,6] and Hiroto Komano[1]

1 Department of Neuroscience, School of Pharmacy, Iwate Medical University, Morioka, Japan
2 Department of Alzheimer's Disease Research, National Center for Geriatrics and Gerontology, Aichi, Japan
3 Department of Demyelinating Disease and Aging, National Institute of Neuroscience, Tokyo, Japan
4 Institute of Medical Science, St. Marianna University School of Medicine, Kawasaki, Japan
5 Choju Medical Institute and Fukushimura Hospital, Toyohashi, Japan
6 Misato Marine Hospital, Kochi, Japan

Keywords
amyloid β-protein; E3 ubiquitin ligase; nicastrin; presenilin; γ-secretase

Correspondence
H. Komano, Department of Neuroscience, School of Pharmacy, Iwate Medical University, 2-1-1 Nishitokuta, Yahaba, Shiwa, Iwate 028-3694, Japan
Fax: +81 19 698 1864
Tel: +81 19 651 5111, extn 5210
E-mail: hkomano@iwate-med.ac.jp

***Present address**
Department of Biology, Faculty of Sciences, Kyushu University Graduate School, Fukuoka, Japan

(Received 13 January 2009, revised 2 August 2009, accepted 6 August 2009)

doi:10.1111/j.1742-4658.2009.07264.x

The presenilin complex, consisting of presenilin, nicastrin, anterior pharynx defective-1 and presenilin enhancer-2, constitutes γ-secretase, which is required for the generation of amyloid β-protein. In this article, we show that Synoviolin (also called Hrd1), which is an E3 ubiquitin ligase implicated in endoplasmic reticulum-associated degradation, is involved in the degradation of endogenous immature nicastrin, and affects amyloid β-protein generation. It was found that the level of immature nicastrin was dramatically increased in *synoviolin*-null cells as a result of the inhibition of degradation, but the accumulation of endogenous presenilin, anterior pharynx defective-1 and presenilin enhancer-2 was not changed. This was abolished by the transfection of exogenous Synoviolin. Moreover, nicastrin was co-immunoprecipitated with Synoviolin, strongly suggesting that nicastrin is the substrate of Synoviolin. Interestingly, amyloid β-protein generation was increased by the overexpression of Synoviolin, although the nicastrin level was decreased. Thus, Synoviolin-mediated ubiquitination is involved in the degradation of immature nicastrin, and probably regulates amyloid β-protein generation.

Structured digital abstract

- MINT-7255352: *Synoviolin* (uniprotkb:Q9DBY1) *physically interacts* (MI:0915) with *NCT* (uniprotkb:P57716) by *anti tag coimmunoprecipitation* (MI:0007)
- MINT-7255377: *Ubiquitin* (uniprotkb:P62991) *physically interacts* (MI:0915) with *NCT* (uniprotkb:P57716) by *anti bait coimmunoprecipitation* (MI:0006)
- MINT-7255363: *NCT* (uniprotkb:P57716) *physically interacts* (MI:0915) with *Synoviolin* (uniprotkb:Q9DBY1) by *anti bait coimmunoprecipitation* (MI:0006)

Introduction

Amyloid β-protein (Aβ), which is the major component of senile plaques in the brains of patients with Alzheimer's disease, is generated from the amyloid precursor protein (APP) through its sequential proteolytic

Abbreviations
Aβ, amyloid β-protein; APH-1, anterior pharynx defective-1; APP, β-amyloid precursor protein; CTF, C-terminal fragment; ER, endoplasmic reticulum; NCT, nicastrin; NTF, N-terminal fragment; PEN-2, presenilin enhancer-2; PS, presenilin.

cleavage catalyzed by β- and γ-secretases [1]. β-Secretase has been identified as a membrane-tethered aspartyl protease [2]. γ-Secretase activity is attributed to the presenilin (PS) complex, which is composed of four transmembrane proteins: PS, nicastrin (NCT), presenilin enhancer-2 (PEN-2) and anterior pharynx defective-1 (APH-1) (collectively named PS cofactors in this study) (reviewed in [3]). Full-length PS is endoproteolytically processed into two fragments: the N-terminal fragment (NTF) and the C-terminal fragment (CTF) [4]. The processed PS resides in the γ-secretase complex (reviewed in [3]). Endogenous PS, NCT, PEN-2 and APH-1 are mainly localized in the endoplasmic reticulum (ER) and Golgi [5], and the properly assembled complex is transported through the secretory pathway to localize predominantly in the Golgi and then at the cell surface [6,7].

NCT is a type I transmembrane protein that possesses many potential glycosylation sites within its large ectodomain [8]. Several studies have established that three principal forms of NCT exist in cells: the unglycosylated, nascent protein (~ 80 kDa); an immature N-linked glycosylated species (immature NCT, ~ 110 kDa); and a mature N-linked isoform (mature NCT, ~ 150 kDa) which is formed after entering the Golgi apparatus [9]. The mature NCT associates with active γ-secretase [10] and, importantly, PS is required for the full post-translational generation of this mature NCT species [9]. In addition, NCT is critical for the stability and trafficking of other γ-secretase components, and NCT affects Aβ production [11].

Interestingly, the cellular level of PS is tightly limited [12]. Excess PS cofactors which fail to reside in the complex, such as full-length PS, mostly undergo ubiquitin/proteasome-mediated degradation, although the precise mechanism of elimination of excess cofactors is not fully understood [12].

Ubiquitination is required for proteasome-mediated degradation, although, recently, accumulating evidence has shown that ubiquitin has multiple functions, including intracellular trafficking (reviewed in [13]), which is accomplished through the sequential actions of enzymes: an activating enzyme (E1), a conjugating enzyme (E2) and a ligase (E3) (reviewed in [14]). Of the three enzymes, E3 enzymes are the key determining factors in substrate protein selection. Synoviolin, a representative of ER-resident E3 ubiquitin ligase, is a mammalian homolog of yeast Hrd1 [15]. Synoviolin is also a pathogenic factor in rheumatoid arthritis [16], and is involved in ER-associated degradation [17]. The substrates of Synoviolin were found to include polyglutamine-expanded huntingtin [18], the tumor suppressor gene p53 [19] and Parkin-associated endothelin receptor-like receptor [20].

In this study, we addressed whether Synoviolin is involved in the degradation of PS cofactors using *synoviolin*-null cells, as PS cofactors undergo the ubiquitin/proteasome pathway. We report that Synoviolin is involved in the degradation of immature NCT and regulates Aβ generation.

Results

Accumulation of immature NCT in *synoviolin*-null cells

To investigate whether Synoviolin is involved in the degradation of PS cofactors, we first compared the levels of PS cofactors by immunoblotting between *synoviolin*-null cells and wild-type (wt) cells. As shown in Fig. 1, the level of endogenous immature NCT was found to be markedly increased in *synoviolin*-null cells, compared with wt cells, although endogenous PS, APH-1 and PEN-2 were not changed in *synoviolin*-null cells. Interestingly, the mobilities of immature and mature NCT on the gel in *synoviolin*-null cells were slightly faster than that in wt cells (Fig. 1A). This is probably a result of the difference in the degree of sugar modification, because deglycosylation treatment of NCT in *synoviolin*-null cells resulted in a similar mobility to that in wt cells (Fig. S1, see Supporting Information). We also determined the levels of γ-secretase-unrelated ER protein (calnexin) and cytoskeleton protein (tubulin) in these cells as the internal control proteins. The calnexin and tubulin levels were found to be similar between these cells, confirming that the same amount of protein was loaded in each lane (Fig. 1A). In addition, the observed accumulation of endogenous immature NCT in *synoviolin*-null cells was abolished by exogenously expressed Synoviolin, but not by the expression of Synoviolin C307A mutant lacking E3 ubiquitin ligase activity [21], indicating that the lack of E3 ubiquitin ligase activity of Synoviolin causes the accumulation of immature NCT (Fig. 1B, right panel). As shown in Fig. 1B (left panel), the overexpression of Synoviolin in wt cells decreased both immature and mature NCT levels; however, very interestingly, the expression of Synoviolin C307A mutant in wt cells caused the accumulation of much more immature NCT than mature NCT. Because the C307A mutant inhibits the ubiquitination mediated by endogenous Synoviolin in a dominant-negative manner, as reported previously [21], this result strongly suggests that Synoviolin-mediated ubiquitination is involved in the preferential degradation of immature NCT.

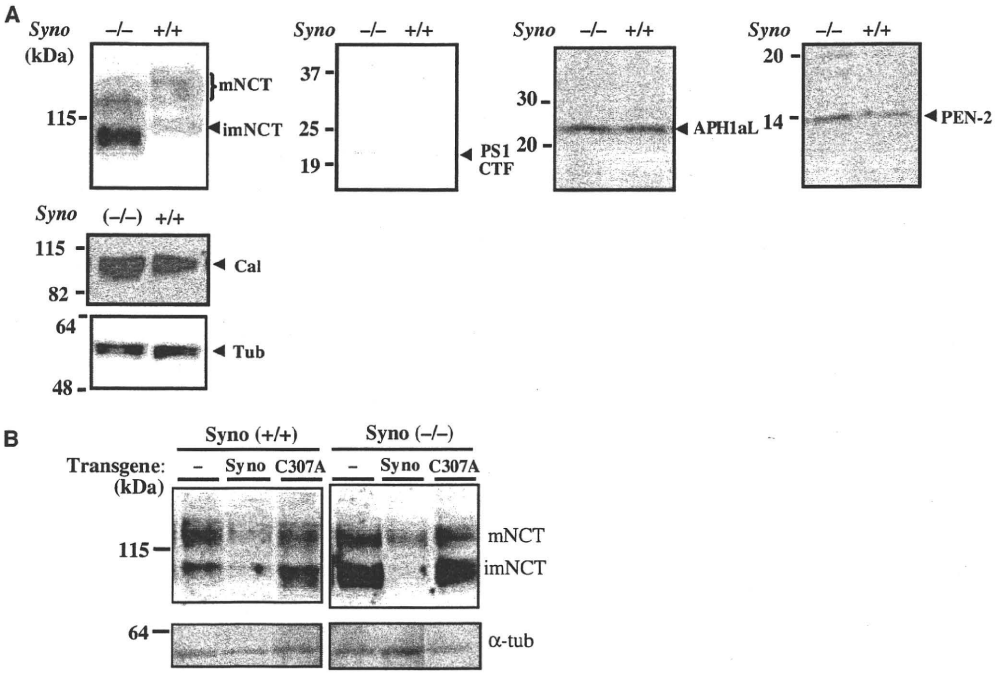

Fig. 1. Accumulation of immature NCT in *synoviolin*-null fibroblasts. (A) The components of the PS complex (NCT, PS-1, APH-1, PEN-2) in the lysate (20 μg) of *synoviolin*-null fibroblasts were detected by immunoblotting with anti-NCT IgG, anti-APH1aL IgG and anti-PEN-2 IgG. Calnexin and α-tubulin in the lysate were also immunodetected as internal markers. −/−, *synoviolin*-null fibroblasts; +/+, wt fibroblasts. (B) NCT in the lysates from wt fibroblasts (left panel) and *synoviolin*-null fibroblasts (right panel), retrovirally expressing Synoviolin or Synoviolin C307A mutant lacking E3 ubiquitin ligase activity, was detected by immunoblotting with anti-NCT IgG. Mutation of the conserved cysteine 307 to alanine in Synoviolin disrupts its ligase activity and this C307A mutant functions in a dominant-negative manner [21]. α-Tubulin in the lysate was also detected as internal marker. imNCT, immature NCT; mNCT, mature NCT; –, mock transfection; Syno, Synoviolin; C307A, Synoviolin C307A mutant; α-tub, α-tubulin.

Effect of Synoviolin on the stability of NCT

Because Synoviolin is an E3 ubiquitin ligase for proteasome-dependent protein degradation, it is most likely that the accumulation of NCT in *synoviolin*-null cells is a result of the suppression of the degradation of NCT. To further investigate this, we next compared the degradation of NCT with time between *synoviolin*-null cells and wt cells. As shown in Fig. 2, western blot analysis of the intracellular degradation of NCT in *synoviolin*-null cells and wt cells following cycloheximide treatment revealed that immature NCT in *synoviolin*-null cells remained stable, as did mature NCT, although, in wt cells, the immature NCT level was preferentially decreased at 10 h after treatment. As a decrease in the immature NCT level seems to include effects of both its maturation and degradation, we further confirmed the degradation of immature NCT in wt cells with treatment by the proteasome inhibitor MG-132. As shown in Fig. 2C, the treatment of wt cells with MG-132 was found to preferentially increase the level of immature NCT compared with that of mature NCT, strongly suggesting that immature NCT is preferentially degraded by the proteasome. Taken together, Synoviolin is most likely to be involved in the preferential degradation of immature NCT via the ubiquitin/proteasome pathway.

Synoviolin interacts with NCT

E3 ligases for ubiquitination confer specificity to the ubiquitin system by directly interacting with the substrate proteins and helping to transfer ubiquitin to them. Therefore, to determine whether NCT is the substrate of Synoviolin, we determined whether Synoviolin interacts with NCT. As shown in Fig. 3, immature NCT was coimmunoprecipitated with anti-FLAG IgG and, in addition, Synovolin was coimmunoprecipitated with anti-NCT IgG when FLAG-tagged Synoviolin and NCT were coexpressed in *synoviolin*-null cells. These results indicate that Synoviolin interacts

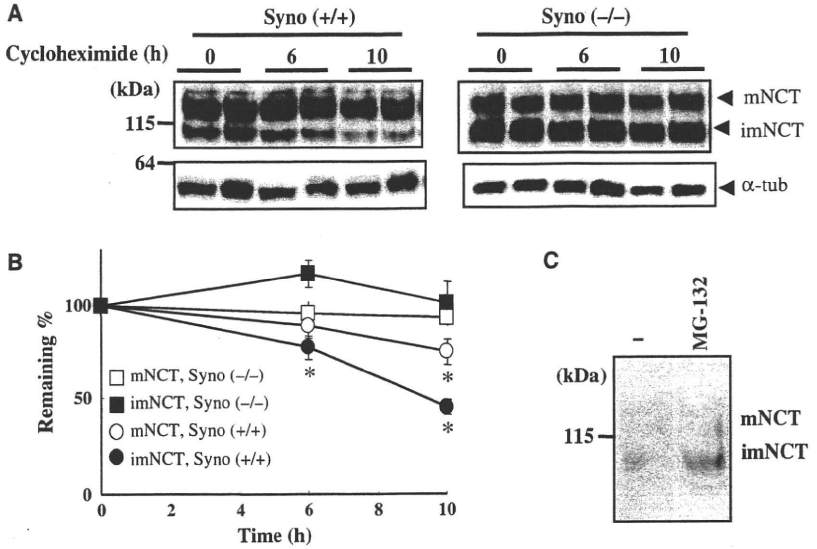

Fig. 2. Degradation of NCT in *synoviolin*-null and wt fibroblasts. (A) *synoviolin*-null and wt fibroblasts were treated with 20 μg·mL^{-1} cycloheximide and harvested at the times indicated. NCT in RIPA-solubilized lysates (10 μg) was detected by immunoblotting with anti-NCT antibody. α-Tubulin in the lysates was also immunodetected as an internal control for a stable protein. Each sample was duplicated. imNCT, immature NCT; mNCT, mature NCT; α-Tub, α-tubulin. (B) The intensities of the bands corresponding to immature NCT and mature NCT in (A) were densitometrically quantified using a luminescent image analyzer LAS-3000 (Fuji Photo Film Co., Ltd., Tokyo, Japan). NCT levels remaining at each time point were calculated as a percentage of the intensity at time zero. Each value is the average of four independent experiments. Asterisk indicates significant differences from time zero [significant difference at $P < 0.05$ (Student's *t*-test)]. (C) Wt fibroblasts were treated with 10 μM MG-132 for 10 h, and NCT in the RIPA-solubilized lysates (10 μg) was detected by immunoblotting with anti-NCT antibody. –, cells treated without MG-132.

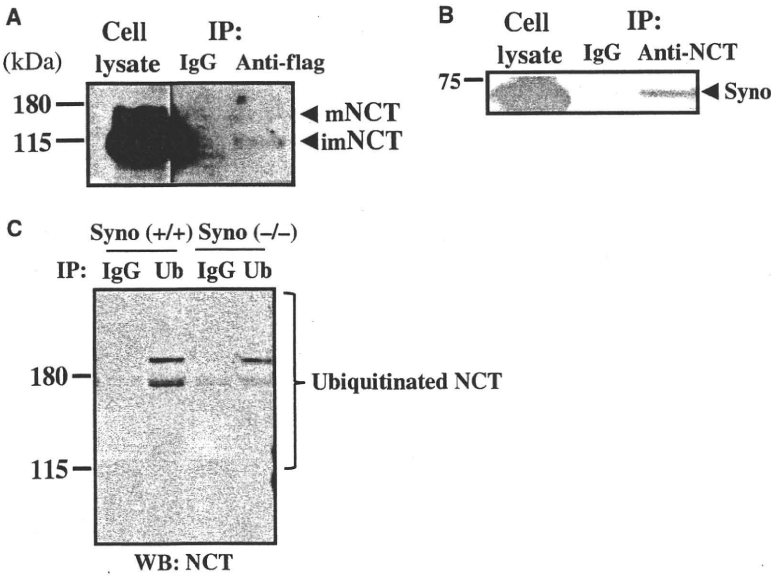

Fig. 3. Synoviolin interacts with NCT. (A) The cell lysates of *synoviolin*-null fibroblasts transiently coexpressing FLAG-tagged Synoviolin and NCT were immunoprecipitated with anti-FLAG antibody and immunodetected with anti-NCT antibody. (B) The same cell lysates were immunoprecipitated with anti-NCT antibody and then immunodetected with anti-Synoviolin antibody. (C) After *synoviolin*-null and wt fibroblasts transiently transfected with NCT had been treated with cycloheximide and lactacystin for 8 h, the cells were harvested. The RIPA-solubilized lysates (1 mg) were immunoprecipitated with anti-ubiquitin mouse antibody (mouse IgG for control) and then immunodetected with anti-NCT antibody. IP, immunoprecipitation; WB, western blot.

with immature NCT. In addition, the degree of ubiquitination of NCT in wt cells was also found to be slightly higher than that in *synoviolin*-null cells (Fig. 3C). However, it was also noted that NCT was slightly ubiquitinated even in *synoviolin*-null cells. Therefore, it is most likely that NCT is a substrate of Synoviolin, but the other E3 ubiquitin ligase also appears to ubiquitinate NCT.

Detection of NCT on the cell surface in *synoviolin*-null cells

Only mature NCT goes to the cell surface, and immature NCT stays within the cells, as reported previously [6,22]. As the level of immature NCT was greatly increased and the molecular weight of NCT was changed slightly in *synoviolin*-null cells, we investigated whether the cellular localization of NCT was different between *synoviolin*-null cells and wt cells. To determine this, we detected NCT localized at the plasma membrane in *synoviolin*-null cells. For this purpose, we labeled the cell surface proteins with biotin, and then detected the surface-biotinylated NCT by immunoblotting with anti-NCT IgG. As shown in Fig. 4A, we found that both immature and mature NCT were clearly detected on the cell surface in *synoviolin*-null cells, although, in wt cells, only mature NCT was detected on the cell surface. In addition, the mature NCT level on the cell surface was increased in *synoviolin*-null cells (Fig. 4B) [percentage of mature NCT at the cell surface relative to that in the total lysate: 24% (wt) versus 64% (Syn−/−)]. These results indicate that a functional deletion of Synoviolin causes a change in the intracellular trafficking of NCT.

Effect of Synoviolin on the production of Aβ

NCT is one of the essential cofactors of the γ-secretase complex. We therefore investigated the effect of the Synoviolin-mediated degradation of NCT on Aβ generation. In Fig. 5, we measured the Aβ level secreted from wt fibroblasts overexpressing APP [23]. As shown in Fig. 5A, B, the overexpression of Synoviolin enhanced the production of Aβ40 and Aβ42 by about twofold, whereas the secretion of soluble APP was not changed in these cells. Figure 5C also showed that the endogenous NCT level was decreased and the intracellular APP level was not changed by the overexpression of Synoviolin. Previously, the targeting of NCT to the cell surface enhanced Aβ generation, because one of the main Aβ generation sites is likely to be in the cell surface [6]. Therefore, it is possible that the overexpression of Synoviolin enhances the localization of NCT at the cell surface, resulting in an enhancement of Aβ generation. To test this possibility, we measured the level of NCT on the cell membrane. No increase in the cell surface NCT level in cells overexpressing Synoviolin was observed (Fig. 5D).

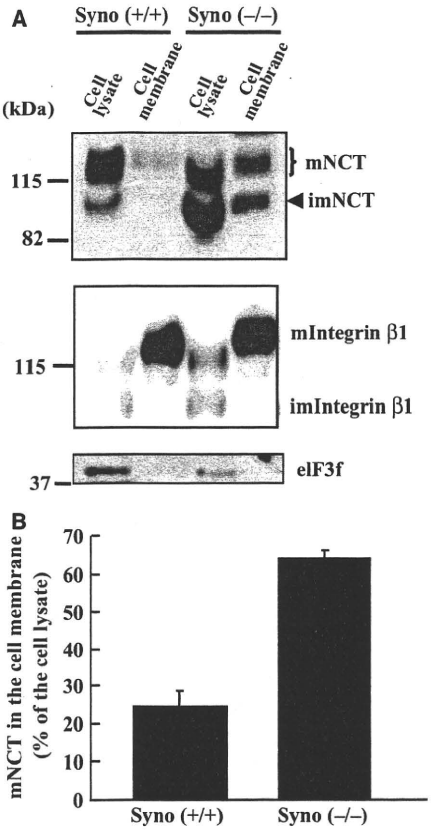

Fig. 4. Cell surface distribution of immature and mature NCT in *synoviolin*-null fibroblasts. (A) Cell surface proteins of *synoviolin*-null and wt fibroblasts were biotinylated as described in Materials and methods. The lysates of surface-biotinylated cells were then incubated with streptavidin–agarose. Total lysate (20 μg) and biotinylated proteins (streptavidin–agarose bound) were immunodetected with anti-NCT IgG, anti-integrin β1 IgG (as a control for the cell surface protein) [22] and anti-eIF3f IgG (as a control for the cytosolic protein) [32]. imNCT, immature NCT; mNCT, mature NCT; m integrin β1, mature integrin β1; im integrin β1, immature integrin β1. (B) Band intensities were densitometrically quantified with a luminescent image analyzer LAS-3000 (Fuji Photo Film Co., Ltd.), and the percentage mature NCT level in the cell membrane relative to that in the total cell lysate was calculated. Data are the average of two independent experiments. The percentage immature NCT level in the cell membrane relative to that in the total cell lysate in *synoviolin*-null cells was 22.0 ± 4.5%.

Discussion

In this study, we showed that Synoviolin is involved in the intracellular degradation of NCT. Of the four γ-secretase components, only NCT was found to be degraded by Synoviolin. In addition, Synoviolin appears to preferentially target immature NCT for degradation, because *synoviolin*-null cells exhibited the accumulation of immature NCT, and the expression of the dominant-negative Synoviolin mutant lacking E3 ubiquitin ligase activity in wt cells caused a greater accumulation of immature NCT than mature NCT.

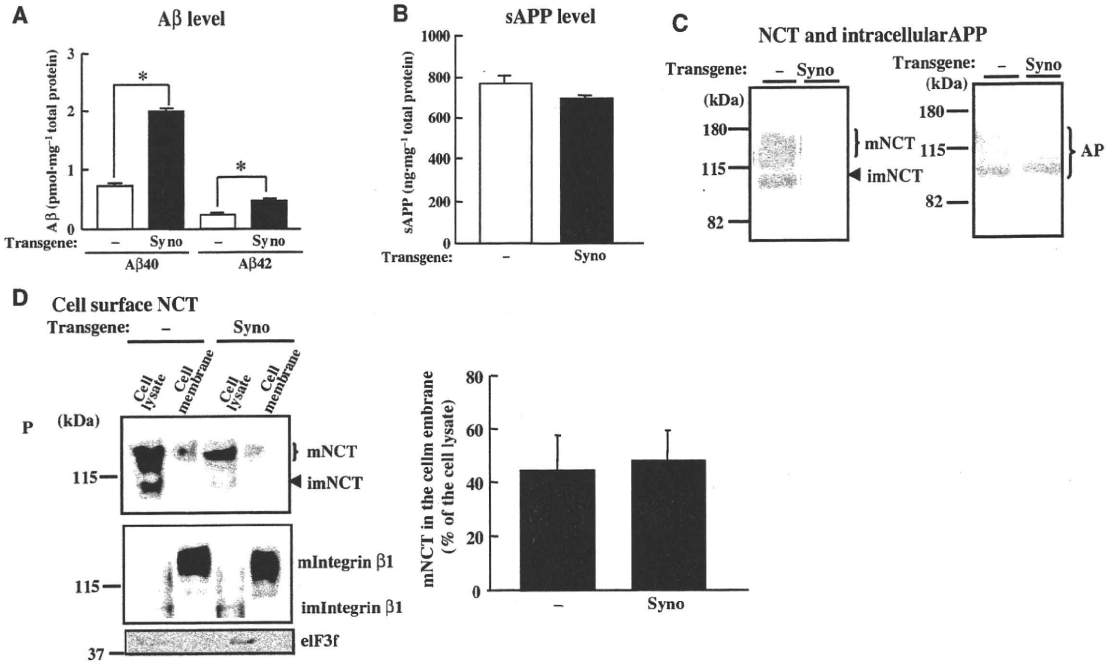

Fig. 5. Effect of the overexpression of Synoviolin on Aβ generation. Wild-type murine fibroblasts expressing APP were retrovirally expressed with Synoviolin. Aβ (A) and soluble APP (B) secreted from the cells during a 96-h culture were detected by ELISA. Values are the means ± SEM of four independent dishes ($n = 4$). Asterisk indicates significant differences from mock [significant difference at $P < 0.01$ (Student's *t*-test)]. (C) NCT and intracellular APP in the cell lysates were immunodetected with anti-NCT IgG and 22C11 respectively. (D) Left panel: cell surface NCT in the mock- or Synovilin-transfected cells was immunodetected as described in Fig. 3. Integrin β1 (as a control for the cell surface protein) and eIF3f (as a control for the cytosolic protein) were also immunodetected. Similar results were obtained from three independent experiments. m integrin β1, mature integrin β1; im integrin β1, immature integrin β1. Right panel: the band intensities were quantified, and the percentage mature NCT level in the cell membrane relative to that of the total cell lysate is shown. Data are the average of three independent experiments. –, mock transfection; Syno, Synoviolin transfection; imNCT, immature NCT; mNCT, mature NCT.

Interestingly, the sugar modification of NCT in *synoviolin*-null cells appeared to be slightly different from that in wt cells. This may suggest that Synovilin-mediated ubiquitination also regulates the trafficking of NCT within the Golgi compartment, because the maturation of the sugar modification of the protein occurs within the Golgi compartment. Recently, there has been an expansion of the recognized roles for ubiquitin in processes other than proteasome-dependent proteolysis, which includes intracellular trafficking (reviewed in [13]). In this regard, it is noteworthy that both immature NCT and mature NCT delivered to the cell surface were increased in *synoviolin*-null cells, although only the mature form of NCT goes to the cell surface in wt cells (Fig. 4). It appears that Synoviolin somehow suppresses the direct delivery of NCT from ER to the cell surface. Previously, it has been shown that Synoviolin increases the membrane localization of huntingtin protein [18], also suggesting that Synoviolin is involved in intracellular trafficking.

We also found that NCT interacts with Synoviolin (Fig. 3), strongly suggesting that NCT is the substrate of Synoviolin. As reported previously, NCT undergoes ubiquitination [24]. We found that the degree of ubiquitination of NCT in wt cells was higher than that in *synoviolin*-null cells. Therefore, NCT is most likely to be a substrate of Synoviolin. However, the other E3 ubiquitin ligase also appears to ubiquitinate NCT, because NCT was ubiqutinated slightly even in *synoviolin*-null cells. Indeed, in *synoviolin*-null cells, NCT started to degrade more than 10 h after cycloheximide treatment (data not shown). Further study of the mechanism underlying NCT degradation mediated by Synoviolin, including an *in vitro* study, is needed.

It was also noted that the overexpression of Synoviolin increased the Aβ level, whereas the cellular level of NCT decreased in transfected cells, because a decreased NCT level would be expected to decrease the Aβ level. Because the levels of full-length APP and soluble APP were not changed (Fig. 5), it is likely that γ-cleavage was increased. As reported previously [25],

the cell membrane NCT level is thought to be more important than the intracellular level of NCT for Aβ generation. Therefore, we investigated whether Synoviolin enhances the cell surface localization of NCT; however, no increase in the cell membrane NCT level in cells transfected with Synoviolin was observed. It has also been shown that the overexpression of SEL-10, that is an E3 ligase for PS1 ubiquitination, causes a decrease in the level of PS1, but an increase in Aβ secretion [26]. This suggests that SEL-10-mediated ubiquitination modulates the PS1 complex in APP processing, although the exact mechanism is not known. Therefore, likewise, Synoviolin-mediated ubiquitination can also regulate Aβ generation, possibly through the modulation of intracellular trafficking. As the overexpression of Synoviolin was suggested to increase γ-cleavage, as mentioned above, the overexpression of Synoviolin, probably through ubiquitination, could promote the trafficking of the PS complex to the site at which γ-cleavage occurs, or activate γ-secretase itself.

In this study, we conclude that Synoviolin is involved in the degradation of immature NCT. We have also shown that the expression of Synoviolin enhances Aβ generation. Further study of the mechanism underlying the enhancement of Aβ generation by Synoviolin will clarify the interaction between the ubiqutination of the PS complex and APP processing.

Materials and methods

Antibodies, reagents and cell lines

A mouse anti-PS1 monoclonal IgG (for the CTF of PS1) was purchased from Chemicon International (Temecula, CA, USA). A rabbit anti-NCT IgG and a mouse NCT monoclonal IgG were purchased from Sigma (St. Louis, MO, USA) and Chemicon International, respectively. MG-132 was purchased from Sigma. A rabbit anti-APH1aL antibody was purchased from COVANCE (Berkeley, CA, USA). Anti-PEN-2 IgM was provided by Dr Thinakaran [27,28]. Anti-α-tubulin and anti-calnexin IgG were purchased from Santa Cruz Biotechnology, Inc. (Santa Cruz, CA, USA). Anti-APP N-terminal antibody 22C11 was purchased from Sigma. Anti-HRD1 (Synoviolin) C-terminal antibody was purchased from ABGENT (San Diego CA, USA). Anti-eIF3f was purchased from Rockland Inc. (Gilbertsville, PA, USA). Anti-integrin β1 antibody was purchased from BD Biosciences (San Jose, CA, USA). Monoclonal antibody against mono- and polyubiquitin was purchased from BIOMOL (Plymouth Meeting, PA, USA). Synoviolin-null murine fibroblasts [29] and murine fibroblasts overexpressing human APP were cultured in Dulbecco's modified Eagle's medium (DMEM; Wako Pure Chemical Industries, Ltd., Osaka, Japan) containing 10% fetal bovine serum.

Plasmids and retrovirus-mediated infection

PMX-Synoviolin was generated as described previously [16]. cDNA encoding Synoviolin C307A mutant was generated by overlap PCR using the following primers: 5′-AAATGTGGTTGGCGGGCAGTCTCTTGGC-3′ and 5′-ACTGCCCGCCAACCACATTTTCC-3′. The PCR product was verified by sequencing. The retrovirus-mediated infection was carried out as reported previously [30].

Cycloheximide treatment

Cells (5×10^5) plated on 60 mm tissue culture dishes were grown for 24 h; cycloheximide was then added to a final concentration of 20 $\mu g \cdot mL^{-1}$. At various times after the addition of cycloheximide, the cells were harvested and lysed in RIPA buffer (150 mM NaCl, 10 mM Tris/HCl pH 7.5, 1% Nonidet P-40, 0.1% SDS and 0.2% sodium deoxycholate) containing a protease inhibitor cocktail.

Immunoprecipitation, immunoblotting and ELISA

Cultured cells were lysed in RIPA buffer containing a protease inhibitor cocktail. The solubilized proteins were subjected to immunoprecipitation as described previously [31]. The precipitated proteins were resolved by SDS-PAGE on 4–20% gel for the detection of PS and NCT. Immunoblotting was performed as reported previously [31]. ELISAs for Aβ and soluble APP were performed using a βAmyloid ELISA kit (Wako Pure Chemical Industries, Ltd., Osaka, Japan) and human soluble APP ELISA kit (IBL Co., Ltd., Nagoya, Japan), respectively.

Cell surface biotinylation

Cell surface biotinylation was carried out using a cell surface protein isolation kit (Pierce, Rockford, IL, USA). The cells were grown in four 10 cm tissue culture dishes, and washed twice with ice-cold NaCl/P_i. The cells were incubated in 10 mL of ice-cold sulfosuccinimidy-2-(biotinamido)-ethyl-1,3-dithiopropionate (0.25 $mg \cdot mL^{-1}$) in ice-cold NaCl/P_i for 30 min at 4 °C, and then 500 μL of the quenching solution were added to each dish to quench the reaction. The cells were scraped and washed twice with Tris-buffered saline (TBS) (10 mM Tris/HCl pH 7.5, 150 mM NaCl) and lysed in lysis buffer containing protease inhibitors. Each lysate was incubated with streptavidin–agarose beads at 4 °C for 60 min, and the captured proteins were eluted with 50 mM dithiothreitol in Laemmli's SDS sample buffer.

Acknowledgements

We thank Dr Gopal Thinakaran for providing anti-PEN-2 IgG. This study was supported in part by a grant-in-aid for scientific research from the Ministry of Education, Culture, Sports, Science and Technology of Japan, and by a grant from the Ministry of Health, Labor and Welfare of Japan. We thank Dr Paul Langman for assistance with the English.

References

1 Selkoe DJ (2002) Deciphering the genesis and fate of amyloid β-protein yields novel therapies for Alzheimer disease. *J Clin Invest* **110**, 1375–1381.
2 Vassar R, Bennett BD, Babu-Khan S, Kahn S, Mendiaz EA, Denis P, Teplow DB, Ross S, Amarante P, Loeloff R *et al.* (1999) β-Secretase cleavage of Alzheimer's amyloid precursor protein by the transmembrane aspartic protease BACE. *Science* **286**, 735–741.
3 De Strooper B (2003) Aph-1, Pen-2, and Nicastrin with Presenilin generate an active γ-Secretase complex. *Neuron* **38**, 9–12.
4 Thinakaran G, Borchelt DR, Lee MK, Slunt HH, Spitzer L, Kim G, Ratovitsky T, Davenport F, Nordstedt C, Seeger M *et al.* (1996) Endoproteolysis of presenilin 1 and accumulation of processed derivatives in vivo. *Neuron* **17**, 181–190.
5 Gu Y, Chen F, Sanjo N, Kawarai T, Hasegawa H, Duthie M, Li W, Ruan X, Luthra A, Mount HT *et al.* (2003) APH-1 interacts with mature and immature forms of presenilins and nicastrin and may play a role in maturation of presenilin–nicastrin complexes. *J Biol Chem* **278**, 7374–7380.
6 Kaether C, Lammich S, Edbauer D, Ertl M, Rietdorf J, Capell A, Steiner H & Haass C (2002) Presenilin-1 affects trafficking and processing of βAPP and is targeted in a complex with nicastrin to the plasma membrane. *J Cell Biol* **158**, 551–561.
7 Kim SH, Yin YI, Li YM & Sisodia SS (2004) Evidence that assembly of an active γ-secretase complex occurs in the early compartments of the secretory pathway. *J Biol Chem* **279**, 48615–48619.
8 Yu G, Nishimura M, Arawaka S, Levitan D, Zhang L, Tandon A, Song YQ, Rogaeva E, Chen F, Kawarai T *et al.* (2000) Nicastrin modulates presenilin-mediated notch/glp-1 signal transduction and βAPP processing. *Nature* **407**, 48–54.
9 Leem JY, Vijayan S, Han P, Cai D, Machura M, Lopes KO, Veselits ML, Xu H & Thinakaran G (2002) Presenilin 1 is required for maturation and cell surface accumulation of nicastrin. *J Biol Chem* **277**, 19236–19240.
10 Kimberly WT, LaVoie MJ, Ostaszewski BL, Ye W, Wolfe MS & Selkoe DJ (2002) Complex N-linked glycosylated nicastrin associates with active γ-secretase and undergoes tight cellular regulation. *J Biol Chem* **277**, 35113–35117.
11 Zhang YW, Luo WJ, Wang H, Lin P, Vetrivel KS, Liao F, Li F, Wong PC, Farquhar MG, Thinakaran G *et al.* (2005) Nicastrin is critical for stability and trafficking but not association of other presenilin/γ-secretase components. *J Biol Chem* **280**, 17020–17026.
12 Ratovitski T, Slunt HH, Thinakaran G, Price DL, Sisodia SS & Borchelt DR (1997) Endoproteolytic processing and stabilization of wild-type and mutant presenilin. *J Biol Chem* **272**, 24536–24541.
13 Mukhopadhyay D & Riezman H (2007) Proteasome-independent functions of ubiquitin in endocytosis and signaling. *Science* **315**, 201–205.
14 Pickart CM (2004) Back to the future with ubiquitin. *Cell* **116**, 181–190.
15 Schulze A, Standera S, Buerger E, Kikkert M, van Voorden S, Wiertz E, Koning F, Kloetzel PM & Seeger M (2005) The ubiquitin-domain protein HERP forms a complex with components of the endoplasmic reticulum associated degradation pathway. *J Mol Biol* **354**, 1021–1027.
16 Amano T, Yamasaki S, Yagishita N, Tsuchimochi K, Shin H, Kawahara K, Aratani S, Fujita H, Zhang L, Ikeda R *et al.* (2003) Synoviolin/Hrd1, an E3 ubiquitin ligase, as a novel pathogenic factor for arthropathy. *Genes Dev* **17**, 2436–2449.
17 Christianson JC, Shaler TA, Tyler RE & Kopito RR (2008) OS-9 and GRP94 deliver mutant alpha1-antitrypsin to the Hrd1-SEL1L ubiquitin ligase complex for ERAD. *Nat Cell Biol* **10**, 272–282.
18 Yang H, Zhong X, Ballar P, Luo S, Shen Y, Rubinsztein DC, Monteiro MJ & Fang S (2007) Ubiquitin ligase Hrd1 enhances the degradation and suppresses the toxicity of polyglutamine-expanded huntingtin. *Exp Cell Res* **313**, 538–550.
19 Yamasaki S, Yagishita N, Sasaki T, Nakazawa M, Kato Y, Yamadera T, Bae E, Toriyama S, Ikeda R, Zhang L *et al.* (2007) Cytoplasmic destruction of p53 by the endoplasmic reticulum-resident ubiquitin ligase 'Synoviolin'. *EMBO J* **26**, 113–122.
20 Omura T, Kaneko M, Onoguchi M, Koizumi S, Itami M, Ueyama M, Okuma Y & Nomura Y (2008) Novel functions of ubiquitin ligase HRD1 with transmembrane and proline-rich domains. *J Pharmacol Sci* **106**, 512–519.
21 Gao B, Lee SM, Chen A, Zhang J, Zhang DD, Kannan K, Ortmann RA & Fang D (2008) Synoviolin promotes IRE1 ubiquitination and degradation in synovial fibroblasts from mice with collagen-induced arthritis. *EMBO Rep* **9**, 480–485.
22 Zou K, Hosono T, Nakamura T, Shiraishi H, Maeda T, Komano H, Yanagisawa K & Michikawa M (2008) Novel role of presenilins in maturation and transport of integrin β1. *Biochemistry* **47**, 3370–3378.

23 Sai X, Kokame K, Shiraishi H, Kawamura Y, Miyata T, Yanagisawa K & Komano H (2003) The ubiquitin-like domain of Herp is involved in Herp degradation, but not necessary for its enhancement of amyloid beta-protein generation. *FEBS Lett* **553**, 151–156.
24 He G, Qing H, Tong Y, Cai F, Ishiura S & Song W (2007) Degradation of nicastrin involves both proteasome and lysosome. *J Neurochem* **101**, 982–992.
25 Morais VA, Leight S, Pijak DS, Lee VM & Costa J (2008) Cellular localization of Nicastrin affects amyloid β species production. *FEBS Lett* **582**, 427–433.
26 Li J, Pauley AM, Myers RL, Shuang R, Brashler JR, Yan R, Buhl AE, Ruble C & Gurney ME (2002) SEL-10 interacts with presenilin 1, facilitates its ubiquitination, and alters A-beta peptide production. *J Neurochem* **82**, 1540–1548.
27 Araki W, Takahashi-Sasaki N, Chui DH, Saito S, Takeda K, Shirotani K, Takahashi K, Murayama KS, Kametani F, Shiraishi H *et al.* (2008) A family of membrane proteins associated with presenilin expression and γ-secretase function. *FASEB J* **22**, 819–827.
28 Luo WJ, Wang H, Li H, Kim BS, Shah S, Lee HJ, Thinakaran G, Kim TW, Yu G & Xu H (2003) PEN-2 and APH-1 coordinately regulate proteolytic processing of presenilin 1. *J Biol Chem* **278**, 7850–7854.
29 Yagishita N, Ohneda K, Amano T, Yamasaki S, Sugiura A, Tsuchimochi K, Shin H, Kawahara K, Ohneda O, Ohta T *et al.* (2005) Essential role of synoviolin in embryogenesis. *J Biol Chem* **280**, 7909–7916.
30 Komano H, Shiraishi H, Kawamura Y, Sai X, Suzuki R, Serneels L, Kawaichi M, Kitamura T & Yanagisawa K (2002) A new functional screening system for identification of regulators for the generation of amyloid β-protein. *J Biol Chem* **277**, 39627–39633.
31 Sudoh S, Kawamura Y, Sato S, Wang R, Saido TC, Oyama F, Sakaki Y, Komano H & Yanagisawa K (1998) Presenilin 1 mutations linked to familial Alzheimer's disease increase the intracellular levels of amyloid beta-protein 1–42 and its N-terminally truncated variant(s) which are generated at distinct sites. *J Neurochem* **71**, 1535–1543.
32 Lagirand-Cantaloube J, Offner N, Csibi A, Leibovitch MP, Batonnet-Pichon S, Tintignac LA, Segura CT & Leibovitch SA (2008) The initiation factor eIF3-f is a major target for atrogin1/MAFbx function in skeletal muscle atrophy. *EMBO J* **27**, 1266–1276.

Supporting information

The following supplementary material is available:
Fig. S1. Deglycosylation of NCT.

This supplementary material can be found in the online version of this article.

Please note: As a service to our authors and readers, this journal provides supporting information supplied by the authors. Such materials are peer-reviewed and may be re-organized for online delivery, but are not copy-edited or typeset. Technical support issues arising from supporting information (other than missing files) should be addressed to the authors.

BJ www.biochemj.org

BJ Metabolism

Biochem. J. (2009) 421, 293–299 (Printed in Great Britain) doi:10.1042/BJ20090286

Dynamic aspects of ascorbic acid metabolism in the circulation: analysis by ascorbate oxidase with a prolonged *in vivo* half-life

Emiko KASAHARA*[1], Misato KASHIBA†, Mika JIKUMARU*, Daisuke KURATSUNE*, Kumi ORITA*, Yurika YAMATE*, Kenjiro HARA*, Atsuo SEKIYAMA*, Eisuke F. SATO* and Masayasu INOUE*

*Department of Biochemistry and Molecular Pathology, Osaka City University Medical School, 1-4-3 Asahimachi, Abeno, Osaka 545-8585, Japan, and †School of Bionics, Tokyo University of Technology, 1401-1 Katakura, Hachioji, Tokyo 192-0982, Japan

Because AA (L-ascorbic acid) scavenges various types of free radicals to form MDAA (monodehydroascorbic acid) and DAA (dehydroascorbic acid), its regeneration from the oxidized metabolites is critically important for humans and other animals that lack the ability to synthesize this antioxidant. To study the dynamic aspects of AA metabolism in the circulation, a long acting AOase (ascorbate oxidase) derivative was synthesized by covalently linking PEG [poly(ethylene glycol)] to the enzyme. Fairly low concentrations of the modified enzyme (PEG–AOase) rapidly decreased AA levels in isolated fresh plasma and blood samples with a concomitant increase in their levels of MDAA and DAA. In contrast, relatively high doses of PEG–AOase were required to decrease the circulating plasma AA levels of both normal rats and ODS (osteogenic disorder Shionogi) rats that lack the ability to synthesize AA. Administration of 50 units of PEG–AOase/kg of body weight rapidly decreased AA levels in plasma and the kidney without affecting the levels in other tissues, such as the liver, brain, lung, adrenal grand and skeletal muscles. PEG–AOase slightly, but significantly, decreased glutathione (GSH) levels in the liver without affecting those in other tissues. Suppression of hepatic synthesis of GSH by administration of BSO [L-buthionin-(*S*,*R*)-sulfoximine] enhanced the PEG–AOase-induced decrease in plasma AA levels. These and other results suggest that the circulating AA is reductively regenerated from MDAA extremely rapidly and that hepatic GSH plays important roles in the regeneration of this antioxidant.

Key words: antioxidant, ascorbate oxidase, ascorbic acid, glutathione, oxidative stress.

INTRODUCTION

The reduced form of AA (ascorbic acid) is a naturally occurring antioxidant that scavenges free radicals to generate its oxidized metabolites, MDAA (monodehydroascorbic acid) and DAA (dehydroascorbic acid) [1–4]. Although plasma levels of the circulating AA in mammals are low (~60 μM), they rapidly undergo oxidation to generate MDAA even under physiological conditions [5–7]. Therefore oxidized metabolites of AA should be reductively regenerated from MDAA and DAA particularly in humans and some mammals that lack the ability to synthesize AA [8]. Because AA synthesis in most animals is restricted to the liver [9–11], AA, MDAA and DAA should be metabolized via inter-organ co-operation to maintain steady-state levels of AA in plasma and tissues [7,12]. Concentrations of AA in cells and tissues are higher than those in plasma by ~2 orders of magnitude. In this context, two types of transport systems for AA and DAA have been reported with mammals, one is the SVCT (Na^+-AA cotransport system) [13–17] and the other is the GLUT (glucose transporter), responsible for the facilitated transport of glucose and DAA [18]. When transported into cells, DAA is enzymatically reduced to AA at the expense of either GSH, thioredoxin or NAD(P)H [19–23]. Because AA does not serve as a substrate for GLUT, AA regenerated from DAA inside cells is kept at high concentrations by a metabolic sink mechanism [24]. Thus cellular activities of SVCT, GLUT and reducing enzymes for MDAA and DAA might determine the steady-state levels of AA in plasma and tissues of animals that lack the activity to synthesize AA; however, the dynamic aspects of transport and metabolism of AA and its oxidized metabolites *in vivo* remain to be elucidated.

In the present study we synthesized PEG [poly(ethylene glycol)]-AOase (ascorbate oxidase), an AA oxidase derivative with a prolonged *in vivo* half-life. Intravenously administered PEG–AOase effectively oxidizes plasma AA to MDAA in a dose-dependent manner. The present study describes the effect of PEG–AOase on plasma and tissue levels of AA, MDAA and DAA in control, STZ (streptozotocin)-treated diabetic rats and ODS (osteogenic disorder Shionogi) rats that lack the ability to synthesize AA [25,26]. The results suggest for the first time that the circulating AA is reductively regenerated extremely rapidly by using hepatic GSH.

MATERIALS AND METHODS

Chemicals

GSH and DTNB [5,5′-dithiobis-(2-nitrobenzoic acid)] were purchased from Wako Pure Chemicals. AOase (EC 1.10.3.3) from cucurbita species, AA, glutathione reductase, DTC (diethyldithiocarbamate), DTPA (diethylenetriamine pentaacetic acid) and STZ were purchased from Sigma. Activated PEG (MW = 10000 Da) was obtained from Seikagaku Kogyo. All other reagents used were the highest grade commercially available.

Animals

Male Wistar rats (8–9 weeks old) obtained from SLC (Shizuoka, Japan) were fed laboratory chow and water *ad libitum* and used for experiments without prior fasting. Unless otherwise stated, they were used for the experiments as normal animals. We also

Abbreviations used: AA, ascorbic acid; AOase, ascorbate oxidase; DAA, dehydroascorbic acid; DTC, diethyldithiocarbamate; DTPA, diethylenetriamine pentaacetic acid; ESR, electron spin resonance; GLUT, glucose transporter; MDAA, monodehydroascorbic acid; ODS, osteogenic disorder Shionogi; PEG, poly(ethylene glycol); STZ, streptozotocin; SVCT, Na^+-AA cotransport system; TCA, trichloroacetic acid.

[1] To whom correspondence should be addressed (email kasahara@med.osaka-cu.ac.jp).

used ODS rats, which lack the ability to synthesize AA, and STZ-induced hyperglycaemic rats. To increase glucose levels in plasma, animals were intravenously administered 50 mg of STZ/kg of body weight 5 days prior to the experiments. The blood glucose levels of STZ-treated rats (435.3 ± 41.3 mg/dl) were higher than those of control animals (117.9 ± 23.0 mg/dl). Male ODS rats (6 weeks old) were obtained from Clea (Osaka, Japan) and allowed free access to normal diet and AA-containing water (1 mg/ml) for 2 weeks. The concentration of AA in the chow was 0.02 %. All experiments were performed according to the Guidelines for Laboratory Animal Care Regulation of Osaka City University Medical School and were approved by the Ethical Committee of our University.

Synthesis of PEG–AOase

Lysyl amino groups of AOase were covalently linked with activated PEG as described previously [27]. Briefly, the reaction mixture contained, in a final volume of 1 ml of 50 mM bicarbonate (pH 10), 250 units of AOase, 250 mg of PEG and 50 mM AA. The mixture was incubated at 37 °C for 3 h and then for 16 h at 4 °C. The incubated mixture was dialysed at 4 °C against 3 litres of 20 mM PBS (pH 7.4). The activities of AOase and PEG–AOase were determined by measuring the rate of AA decrease. The reaction was stopped by adding 5 mM DTC, and the remaining AA was determined. One unit of the enzyme was defined as the amount of the enzyme required for the oxidation of 1 μmol of AA per min at 37 °C and pH 7.4.

Oxidation of AA by PEG–AOase

Under light ether anaesthesia, blood samples were obtained from the abdominal artery in heparinized tubes. To the fresh blood samples was added Tris/HCl (pH 7.4) to give a final concentration of 20 mM to maintain their pH. Plasma samples were obtained after centrifugation of the blood at 10000 *g* at 4 °C for 1 min. Blood and plasma samples were incubated with 20 m-units/ml of PEG–AOase at 37 °C in air. After incubation with the enzyme, the blood and plasma samples were collected in 1 mM DTC- and DTPA-containing tubes to stop further oxidation of AA. Blood samples were immediately centrifuged at 10000 *g* for 30 s. Plasma samples thus obtained were analysed for AA, MDAA and DAA.

Under urethane anaesthesia, rats were injected with various doses of PEG–AOase. At the indicated times, blood samples were collected from the left femoral vein in 1 mM DTC- and DTPA-containing tubes and analysed for AA, MDAA and DAA. Some animals were intravenously injected with 1 mmol of BSO/kg of body weight prior to the administration of PEG–AOase.

Analysis of AA and GSH levels

Fresh plasma samples were mixed with an equivolume of 10 % TCA (trichloroacetic acid). The excised tissues were homogenized using a micro homogenizer (Physcotron; Microtec) in 5 vol. of ice-cold 5 % TCA containing 1 mM DTPA. After centrifugation of the samples at 10000 *g* at 4 °C for 10 min, the acid-soluble fractions were used for the analysis of AA, free thiols and glutathione. AA levels were determined by using HPLC equipped with a Shimazu electrochemical detection system [28,29]. DAA levels were calculated by subtraction of AA levels from total levels of AA in the samples. The total AA level was determined using HPLC analysis after reduction of the acid-soluble fractions with 3.3 mM DTT (dithiothreithol) containing 330 mM K_2HPO_4 for 5 min at room temperature (22 °C) as described previously [30]. Total glutathione (GSH + 2 GSSG) and low-molecular-mass thiols were determined using the method of Tietze [31] and Ellman [32] respectively.

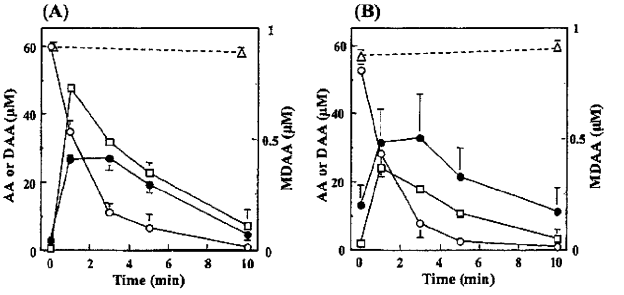

Figure 1 Effect of PEG–AOase on plasma AA levels *in vitro*

Freshly prepared plasma (**A**) or blood (**B**) samples from normal rats were incubated in the presence or absence of 20 m-units of PEG–AOase/ml at 37 °C. At the indicated times, AA (○), MDAA (□) and DAA (●) levels were determined as described in the Materials and methods section. AA levels in the blood and plasma samples remained unchanged after incubation for 10 min in the absence of PEG–AOase (△). Values are means ± S.E.M. ($n = 5$).

ESR (electron spin resonance) analysis

An extracorporeal blood circulation system was established as described previously [33]. Briefly, male Wistar rats were anaesthetized with urethane, and polyethylene tubings (0.60 mm and 0.47 mm in diameter) were inserted into the left femoral artery and vein respectively. The two tubings were connected to an ESR flow cell (200 μl). The flow rate of the blood in the circuit was controlled by a Perista pump at 1 ml/min. Before and after intravenous injection of PEG–AOase, the ESR spectrum of MDAA in the circulation was recorded using a JEOL TES-TE 200 at 37 °C (8 mW of power, 0.079 mT modulation, 334.6 ± 5 mT magnetic field, 5 mT sweep width, 4 min sweep time and a 0.3 s time constant). Concentrations of MDAA were determined by using an external standard based on the signal intensity.

Statistics

Values are expressed as the mean ± S.E.M. derived from 5–15 animals. Statistical analysis was performed using ANOVA followed by a Student's *t* test and the level of significance was $P < 0.05$.

RESULTS

Oxidation of AA by PEG–AOase in isolated plasma and blood

To elucidate the dynamic aspects of AA metabolism in isolated plasma and blood, the effect of PEG–AOase on the plasma levels of AA and its metabolites were analysed *in vitro*. Incubation with PEG–AOase (20 m-units/ml) rapidly decreased AA levels in plasma with a concomitant increase in MDAA and DAA levels (Figure 1A). Then, the increased MDAA and DAA rapidly decreased at similar rates. When incubated with fresh blood, PEG–AOase also decreased plasma levels of AA and increased MDAA and DAA (Figure 1B). The rate of MDAA increase in blood samples was slightly lower than that observed in the experiment with plasma samples. Under identical conditions, the levels of AA in the plasma (59.9 ± 0.88 μM) and blood (57.1 ± 1.50 μM) remained unchanged (57.9 ± 0.64 μM and 60.5 ± 1.65 μM respectively) at least for 10 min in the absence of PEG–AOase.

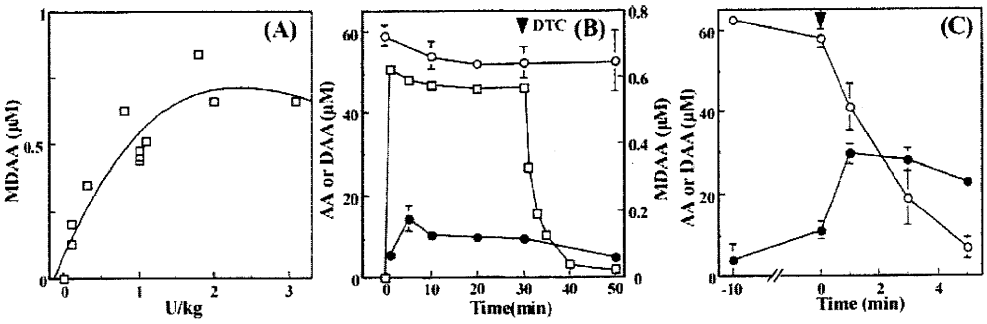

Figure 2 Effect of PEG–AOase on the concentration of AA and its metabolites in the circulation

At 1 min after intravenous administration of various doses of PEG–AOase to normal rats, the levels of the circulating MDAA (□) were determined using the ESR method (**A**) as described in the Materials and methods section. Time-dependent changes in AA (○), MDAA (□) and DAA (●) levels were also measured after administration of 1 unit of PEG–AOase/kg of body weight (**B**). At the indicated time (arrow), the catalytic activity of PEG–AOase was blocked by intravenous administration of 0.1 mmol of DTC/kg of body weight. After 10 min of administration of 1 unit of the enzyme/kg of body weight, blood samples were collected and incubated for 1, 3 and 5 min at 37 °C in air (**C**). Then, plasma levels of AA and DAA were also determined. Values are the means ± S.E.M. ($n = 8 \sim 15$).

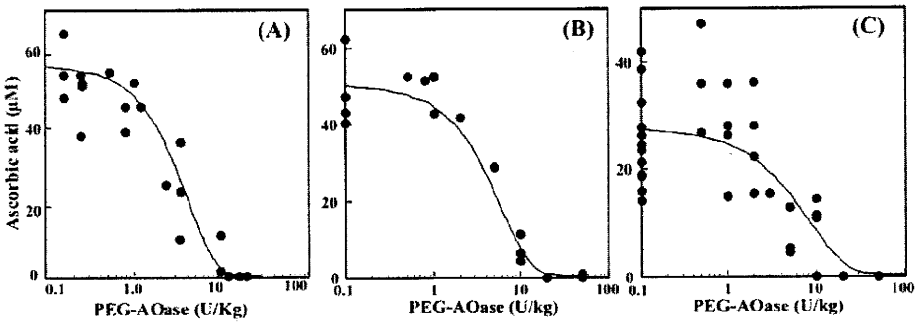

Figure 3 Effect of PEG–AOase on the circulating AA

Various doses of PEG–AOase were injected intravenously into normal (**A**), ODS (**B**) and STZ-treated (**C**) rats. Plasma AA levels in the circulation were determined 2 h after the administration. Other conditions were as in Figure 2. Values are means ± S.E.M. ($n = 5 \sim 11$).

Oxidation of AA by PEG–AOase in the circulation

To elucidate the dynamic aspects of the metabolism and transport of AA in the circulation, the effect of PEG–AOase on the circulating plasma levels of AA and its metabolites were analysed *in vivo* using the ESR blood circulation system as described in the Material and methods section. Intravenous administration of PEG–AOase increased plasma levels of MDAA in a dose-dependent manner (Figure 2A). Figure 2(B) shows the time-dependent changes in AA and its oxidized metabolites in plasma after administration of PEG–AOase. Although PEG–AOase (1 unit/kg of body weight) rapidly increased plasma levels of MDAA in the circulation, no significant decrease was found to occur with circulating AA levels (Figure 2B). The increased MDAA in the circulation rapidly decreased after administration of DTC, a chelating agent for Cu^{2+} to inactivate PEG–AOase, suggesting that PEG–AOase continuously oxidized AA while the generated MDAA rapidly disappeared from the circulation.

Although a fairly high dose (1 unit/kg of body weight) of the enzyme failed to decrease AA levels in the circulation, its plasma levels rapidly decreased after isolation of the blood with a concomitant increase in DAA levels as observed with *in vitro* experiments (Figure 2C). Thus we tested the effect of high doses of the enzyme on AA levels in the circulation (Figure 3). PEG–AOase started to decrease the plasma AA levels in normal rats at doses higher than 2 units/kg of body weight (Figure 3A). At PEG–AOase doses higher than 10 units/kg of body weight, AA levels in the circulation rapidly decreased.

Effects of AA synthesis and GLUT on the circulating AA

To test the possible involvement of *de novo* synthesis of AA in the mechanism for the maintenance of the circulating AA, the effect of the enzyme was also investigated with ODS rats that lack the ability to synthesize AA (Figure 3B). At doses higher than 2 units/kg of body weight, PEG–AOase also decreased plasma AA levels in ODS rats in a similar manner as in normal rats. We also studied the possible involvement of glucose transporters in the regeneration of circulating AA using STZ-induced diabetic rats (Figure 3C). Although steady-state levels of plasma AA in STZ-treated rats (30.74 ± 5.53 μM) were lower than those of control rats (57.41 ± 2.57 μM), the dose-dependency of the PEG–AOase-induced decrease in the circulating AA was similar with the two animal groups.

Effect of a high dose of PEG–AOase on plasma and tissue AA levels

Administration of a high dose of PEG–AOase (50 units/kg of body weight) rapidly diminished circulating AA levels (Figure 4). Although the plasma levels of DAA were elevated by PEG–AOase, the extent of their increase was similar to that of animals that were injected with 1 unit of the enzyme/kg of body weight

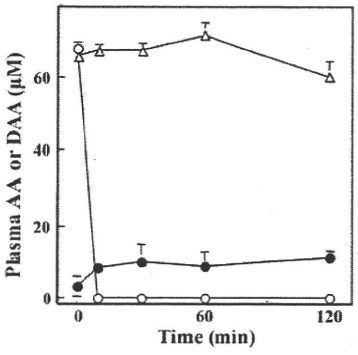

Figure 4 Effect of a high dose of PEG–AOase on the circulating AA and DAA

After intravenous administration of 50 units of PEG–AOase/kg of body weight to normal rats, plasma levels of AA (○, △) and DAA (●) were determined in control (△) and PEG–AOase-treated rats (○, ●). The control animals were treated with the same volume of saline (1 ml/kg of body weight). Values are means ± S.E.M. ($n = 5 \sim 6$).

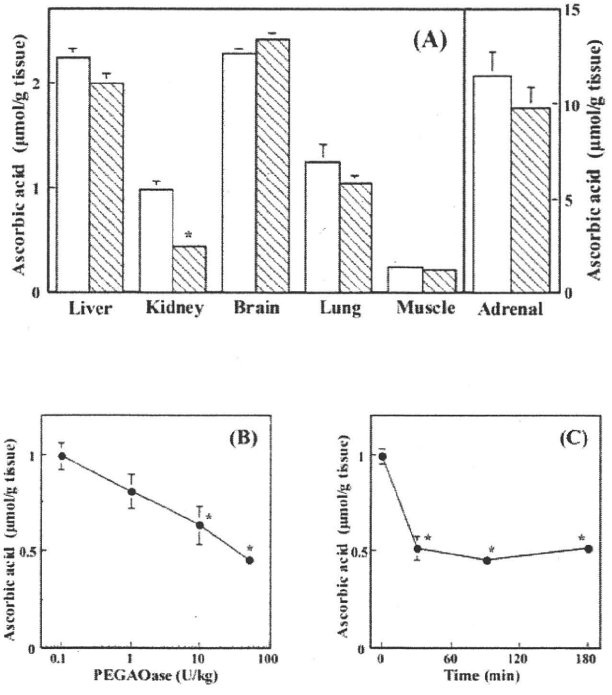

Figure 5 Effect of PEG–AOase on tissue AA levels

PEG–AOase (50 units/kg of body weight) was administered intravenously to normal rats and tissue AA levels were determined after 2 h (**A**) as described in the Materials and methods section. The dose-dependency of the PEG–AOase-induced decrease in renal AA was determined (**B**). Time-dependent changes in renal AA levels were also analysed in animals treated with 50 units of PEG–AOase/kg of body weight (**C**). Values are means ± S.E.M. ($n = 5$). *$P < 0.05$ compared with controls.

(see Figure 2B). Administration of the same doses of the heat-inactivated PEG–AOase had no appreciable effect on the plasma levels of AA and its oxidized metabolites (results not shown). Figure 5 shows the effect of a high dose of PEG–AOase on AA levels in various tissues. Among various tissues examined, AA levels apparently decreased only in the kidney (by approx. 50%). The decrease in renal AA levels depended on the doses of the enzyme (Figure 5B). A high dose of PEG–AOase (50 units/kg

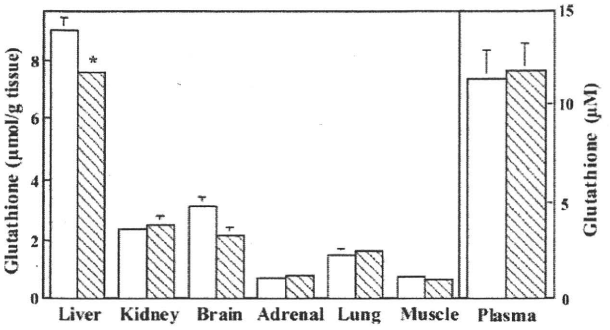

Figure 6 Effect of PEG–AOase on tissue GSH levels

At 2 h after intravenous administration of 50 units of PEG–AOase/kg of body weight to normal rats (hatched columns), total glutathione levels in tissues were determined as described in the Materials and methods section. Control groups (open columns) were administered with 1 ml of saline/kg of body weight. Values are means ± S.E.M. ($n = 5$). *$P < 0.05$ compared with controls.

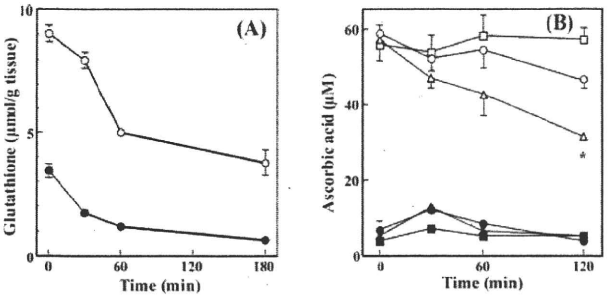

Figure 7 Effect of PEG–AOase on the circulating AA and DAA in BSO-treated animals

After intravenous administration of 1 mmol of BSO/kg of body weight to normal rats, changes in glutathione levels in the liver (○) and kidney (●) were determined (**A**). At 3 h after administration of either saline (○, ●) or BSO (△, ▲), 1 unit of PEG–AOase/kg of body weight was administered to rats. Then, the plasma levels of AA (○, △, □) and DAA (●, ▲, ■) were determined (**B**) as described in the Materials and methods section. Control rats were administered with BSO and saline (□, ■). Most of the glutathione was found to be in the reduced form (GSH). Values are means ± S.E.M. ($n = 5$). *$P < 0.05$ compared with the control.

of body weight) rapidly decreased the renal AA levels by approx. 50%. The decreased AA levels in the kidney remained unchanged for at least 180 min after the administration of the enzymes (Figure 5C).

Role of GSH in the maintenance of the circulating AA

Since GSH is an important cofactor for the reductive regeneration of AA [24], the effects of PEG–AOase on tissue GSH status were studied (Figure 6). Administration of a high dose of PEG–AOase (50 units/kg of body weight) slightly, but significantly, decreased GSH levels in the liver but not in plasma and other tissues, such as the kidney, brain, adrenal gland, lung and gastrocnemius muscle. To get further insights into the relationship between GSH and AA regeneration, effects of PEG–AOase on plasma AA levels were also observed with BSO-treated rats. Administration of BSO markedly decreased GSH levels in the liver and kidney (Figure 7A). Although administration of 1 unit of PEG–AOase/kg of body weight did not appreciably affect plasma AA levels in control rats, the same dose of the enzyme markedly decreased plasma AA levels in BSO-pretreated rats (Figure 7B). The increased levels of plasma DAA in PEG–AOase-treated animals were similar in the control and BSO-treated groups.

DISCUSSION

The present study demonstrates that AA oxidized in the circulation is reductively regenerated extremely rapidly to maintain its steady-state levels in plasma and that hepatic GSH plays an important role in the regeneration mechanism.

It has been well documented that MDAA rapidly undergoes dismutation to form AA and DAA and the resulting DAA rapidly decomposes to di-keto-L-gulonic acid under physiological conditions [2,4]. Although PEG–AOase rapidly oxidized AA to MDAA both in isolated plasma and blood samples, the amounts of MDAA and DAA formed were fairly small as compared with that of the oxidized AA. Furthermore, both MDAA and DAA disappeared at similar rates (a half-life of 4 min) irrespective of the presence of blood cells. Biochemical analysis revealed that DAA spontaneously decomposed with half-lives of 5 and 4 min in PBS and fresh plasma respectively; most DAA as well as AA oxidized by the enzyme *in vitro* was recovered as oxidative metabolites including di-keto-L-gulonic acid (results not shown). Although di-keto-L-gulonic acid is one of the major oxidation products of AA, MDAA and DAA, it undergoes non-enzymic decomposition to form other metabolites including 3,4-dihydroxy-2-oxobutanal [4]. It should be noted that erythrocytes uptake DAA via GLUT and the transported DAA is subsequently reduced intracellularly to AA [34–36]. Previous studies have also revealed that erythrocytes directly reduce extracellular ascorbate radicals [34,37–39]. Because the transient increase of MDAA in PEG–AOase-treated blood was smaller than that in plasma and the rate of DAA disappearance in plasma and blood were similar (see Figure 1), the two mechanisms for AA regeneration by erythrocytes seem to operate minimally, particularly when plasma AA is oxidized rapidly.

Although a fairly high dose of PEG–AOase (1 unit/kg of body weight) oxidized the circulating AA to form MDAA as effectively as in isolated blood and plasma, it failed to decrease the steady-state levels of plasma AA *in vivo* (compare Figures 1 and 2). Assuming 10 ml for the plasma volume of 200 g rats, the initial concentration of the administered enzyme would be approx. 20 m-units/ml of the circulating plasma; this dose of the enzyme would have been sufficient for rapidly oxidizing the AA in isolated plasma (approx. 60 μM). However, the administration of this dose of the enzyme failed to decrease AA levels in the circulation. Under identical conditions, plasma AA levels decreased rapidly only after isolation of the blood samples from the PEG–AOase-induced animals as observed in *in vitro* experiments with fresh plasma (see Figure 2B), suggesting that the administered enzyme continuously oxidized the circulating AA and the oxidized AA metabolite(s) was reductively regenerated to AA extremely rapidly by some unknown mechanism to maintain its steady-state level in plasma.

To investigate the ability of animals to maintain steady-state levels of the circulating AA, we tested the effect of various doses of a long-acting PEG–AOase. The enzyme started to decrease the circulating AA at doses higher than 2 units/kg of body weight in control, ODS and STZ-treated rats. This observation suggests that the activity of animals to regenerate the circulating AA from its oxidized metabolite(s) for the maintenance of its steady-state levels in plasma is as high as 2 μmol/min per kg of body weight.

Because PEG–AOase dose-dependently decreased the circulating AA in control, ODS and STZ-treated rats in a similar fashion, *de novo* synthesis of AA and uptake of DAA by a GLUT system followed by its intracellular reduction may not account for the rapid regeneration of the circulating AA from its oxidized metabolite(s) (particularly when the rate of AA oxidation is high). It should be noted that, although the dose-dependency of the enzyme to decrease the circulating AA in STZ-treated rats was similar to that of control animals, the steady-state levels of plasma AA in the former (30.7 ± 5.5 μM) were significantly lower than those of the latter (57.4 ± 2.6 μM). This observation is consistent with the findings that plasma AA levels in patients with diabetes mellitus are lower than those of healthy subjects [40]. Thus the activity to scavenge toxic free radicals in and around the circulation would be decreased in diabetic subjects. Alternatively, the generation of reactive oxygen species would be increased in diabetic subjects, thereby resulting in low steady-state levels of the circulating AA.

The steady-state levels of AA in the circulation remained unchanged even in the presence of PEG–AOase (1 unit/kg of body weight) sufficient for decreasing AA levels in fresh plasma. Biochemical analysis revealed that PEG–AOase selectively decreased renal AA levels in a dose-dependent manner with a concomitant decrease of the circulating AA (see Figure 5). When the circulating AA was depleted by a high dose of PEG–AOase (50 units/kg of body weight), renal AA levels rapidly decreased by approx. 50% and remained at low levels for 180 min. Assuming 1 g for the renal weight of 200 g rats, approx. 17 nmol of renal AA would have been consumed within 1 min in animals administered with 50 units of the enzyme/kg of body weight. This amount of AA is identical with that of plasma AA that could be filtered by the glomerulus [41]. Since bilateral nephrectomy did not affect plasma levels of AA and administration of PEG–AOase dose-dependently decreased plasma AA levels similarly in control and nephrectomized rats (results not shown), the kidney may not play a major role in the reductive regeneration of AA, although the renal AA level depends on its plasma levels. It is not clear at present why renal AA did not decrease to lower levels than 50% even if extremely high doses of PEG–AOase were administered. It has been well documented that AA and DAA are transferred across plasma membranes of various cells and tissues via active SVCT [42] and bidirectional GLUT systems [43–46] respectively. To our surprise, the levels of AA in liver, brain, lung, muscle and adrenal gland remained unchanged even after depletion of plasma AA (see Figure 5). This observation suggests the presence of a special mechanism that maintains the steady-state levels of cellular AA in these tissues. In contrast, the renal level of AA was affected significantly by PEG–AOase. It should be noted that most low-molecular-mass nutrients filtered by the glomerulus, such as glucose and amino acids, are reabsorbed across renal tubule cells by some transepithelial transport systems in the kidney [41]. Because renal proximal tubules are highly enriched with both SVCT [42] and GLUT [43–46], the filtered AA and DAA would be reabsorbed and transferred to the circulation to maintain their steady-state levels in the kidney and plasma. Thus the renal AA level seems to reflect the balance between the two systems, the one utilized AA within the kidney and the other utilized AA derived from plasma via glomerular filtration (and/or peritubular) mechanism and transepithelial transport to the circulation (salvage system). Depression of plasma AA might decrease not only glomerular filtration of AA (and DAA) but also renal accumulation of the two metabolites. The decreased levels of AA in PEG–AOase-treated animals suggests the importance of the filtered AA and DAA for the maintenance of their steady-state-levels in the kidney. It should be noted that the renal levels of AA remained unchanged after 30 min of PEG–AOase administration. Since most of the nutrients including AA are reabsorbed effectively by renal brush border membranes of proximal tubules, the filtered AA and DAA may not affect their steady-state levels in the lower portions of nephrons than proximal tubules, such as Henle's loop, distal tubules and collecting ducts.

Thus the dynamic aspects of metabolism and transport of AA and DAA at proximal tubules and the lower portion(s) of nephron structures seem to differ; they occur rapidly in the former and slowly in the latter. The possible presence of such zonation of metabolism and transport of AA and DAA within nephron structure should be studied further.

The reductive regeneration of AA from its oxidized forms requires reducing cofactors, such as NAD(P)H and GSH [19,21]. Because both GSH and NAD(P)H are localized ubiquitously with high concentrations, most cells and tissues may have sufficient capacity to catalyse the reductive regeneration of AA. It should be noted, however, that administration of a high dose of PEG–AOase (50 units/kg of body weight) slightly, but significantly, decreased GSH levels in the liver (Figure 6). Under identical conditions, PEG–AOase had no appreciable effect on AA levels in tissues except for the kidney. Thus hepatic GSH might play important roles in the maintenance of the circulating AA. To test this possibility, we investigated the effect of BSO, a specific inhibitor of GSH synthesis, on the steady-state levels of the circulating AA in animals treated with PEG–AOase. When hepatic GSH levels had been decreased by BSO, PEG–AOase (1 unit/kg of body weight) significantly decreased AA levels in the circulation (see Figure 7B). Thus hepatic GSH seems to be responsible, at least in part, for the reductive regeneration of AA from its oxidized metabolite(s) in the circulation. In this context, the presence of a transmembranous enzyme that catalyses the reduction of ascorbate free radicals has been described in hepatocytes, neuronal cells and red blood cells [34,47–49]. It has also been reported that treatment of erythrocytes with *N*-ethylmaleimide at concentrations sufficient for alkylating most intracellular GSH increased the concentration of extracellular ascorbate radicals [38]. Although AA levels in fresh plasma and blood were similarly decreased by a low dose of PEG–AOase, the transient increase of MDAA, but not DAA, was slightly lower in the latter than in the former (see Figure 1). Thus the transmembranous enzyme in the liver and erythrocytes to reduce MDAA to AA may also operate, at least in part, to regenerate the circulating AA. Since the rates of AA decrease by PEG–AOase were similar with isolated blood and plasma samples, hepatic GSH seems to play predominant roles in the regeneration of the circulating AA. A transmembrane mechanism to catalyse the GSH-dependent reduction of MDAA to form AA, similar to that of the NADH-dependent reductase, might operate in the liver. This possibility should be studied further.

Because DAA is unstable and irreversibly decomposed to form di-keto-L-gulonic acid, reductive regeneration of AA from MDAA might be of critical importance for the maintenance of AA levels in the circulation irrespective of the ability of animals to synthesize AA, a potent antioxidant that protects aerobic life from oxidative stress.

AUTHOR CONTRIBUTION

Emiko Kasahara, Misato Kashiba, Mika Jikumaru, Daisuke Kuratsune, Kumi Orita, Yurika Yamate and Kenjiro Hara performed the study. Atsuo Sekiyama and Eisuke Sato contributed to this study with their critical discussion and suggestion. Masayasu Inoue provided most of the ideas of the experiments and his grant supported the study.

FUNDING

This work was supported by the Special Coordination Funds for Promoting Science and Technology from the Ministry of Education, Culture, Sports, Science, and Technology, Japan [project numbers 16590252, 14370062]; and the 21st Century COE Program 'Base to Overcome Fatigue' supported by the Ministry of Education, Culture, Sports, Science, and Technology, Japan.

REFERENCES

1 Niki, E. (1987) Interaction of ascorbate and α-tocopherol. Ann. N Y Acad. Sci. **498**, 186–199
2 Winkler, B. S. (1987) *In vitro* oxidation of ascorbic acid and its prevention by GSH. Biochim. Biophys. Acta **925**, 258–264
3 Frei, B., Stocker, R. and Ames, B. N. (1988) Antioxidant defenses and lipid peroxidation in human blood plasma. Proc. Natl. Acad. Sci. U.S.A. **85**, 9748–9752
4 Nishikawa, Y., Toyoshima, Y. and Kurata, T. (2001) Identification of 3,4-dihydroxy-2-oxo-butanal (L-threosone) as an intermediate compound in oxidative degradation of dehydro-L-ascorbic acid and 2,3-diketo-L-gulonic acid in a deuterium oxide phosphate buffer. Biosci. Biotechnol. Biochem. **65**, 1707–1712
5 Kunitomo, R., Miyauchi, Y. and Inoue, M. (1992) Synthesis of a cytochrome *c* derivative with prolonged *in vivo* half-life and determination of ascorbyl radicals in the circulation of the rat. J. Biol. Chem. **267**, 8732–8738
6 Koyama, K., Takatsuki, K. and Inoue, M. (1994) Determination of superoxide and ascorbyl radicals in the circulation of animals under oxidative stress. Arch. Biochem. Biophys. **309**, 323–328
7 Inoue, M. and Koyama, K. (1994) *In vivo* determination of superoxide and vitamin C radicals using cytochrome *c* and superoxide dismutase derivatives. Methods Enzymol. **234**, 338–343
8 Burns, J. J. (1957) Missing step in man, monkey and guinea pig required for the biosynthesis of L-ascorbic acid. Nature **180**, 553
9 Majumder, P. K., Banerjee, S. K., Roy, R. K. and Chatterjee, G. C. (1973) Effect of insulin on the metabolism of L-ascorbic acid in animals. Biochem. Pharmacol. **22**, 759–761
10 Nishikimi, M. and Yagi, K. (1996) Biochemistry and molecular biology of ascorbic acid biosynthesis. Subcell. Biochem. **25**, 17–39
11 Linster, C. L. and Van Schaftingen, E. (2006) Glucuronate, the precursor of vitamin C, is directly formed from UDP-glucuronate in liver. FEBS J. **273**, 1516–1527
12 Upston, J. M., Karjalainen, A., Bygrave, F. L. and Stocker, R. (1999) Efflux of hepatic ascorbate: a potential contributor to the maintenance of plasma vitamin C. Biochem. J. **342**, 49–56
13 Daruwala, R., Song, J., Koh, W. S., Rumsey, S. C. and Levine, M. (1999) Cloning and functional characterization of the human sodium-dependent vitamin C transporters hSVCT1 and hSVCT2. FEBS Lett. **460**, 480–484
14 Tsukaguchi, H., Tokui, T., Mackenzie, B., Berger, U. V., Chen, X. Z., Wang, Y., Brubaker, R. F. and Hediger, M. A. (1999) A family of mammalian Na^+-dependent L-ascorbic acid transporters. Nature **399**, 70–75
15 Wang, Y., Mackenzie, B., Tsukaguchi, H., Weremowicz, S., Morton, C. C. and Hediger, M. A. (2000) Human vitamin C (L-ascorbic acid) transporter SVCT1. Biochem. Biophys. Res. Commun. **267**, 488–494
16 Liang, W. J., Johnson, D. and Jarvis, S. M. (2001) Vitamin C transport systems of mammalian cells. Mol. Membr. Biol. **18**, 87–95
17 Mackenzie, B., Illing, A. C. and Hediger, M. A. (2008) Transport model of the human Na^+-coupled L-ascorbic acid (vitamin C) transporter SVCT1. Am. J. Physiol. Cell. Physiol. **294**, C451–C459
18 Vera, J. C., Rivas, C. I., Fischbarg, J. and Golde, D. W. (1993) Mammalian facilitative hexose transporters mediate the transport of dehydroascorbic acid. Nature **364**, 79–82
19 Del Bello, B., Maellaro, E., Sugherini, L., Santucci, A., Comporti, M. and Casini, A. F. (1994) Purification of NADPH-dependent dehydroascorbate reductase from rat liver and its identification with 3 α-hydroxysteroid dehydrogenase. Biochem. J. **304**, 385–390
20 May, J. M., Mendiratta, S., Hill, K. E. and Burk, R. F. (1997) Reduction of dehydroascorbate to ascorbate by the selenoenzyme thioredoxin reductase. J. Biol. Chem. **272**, 22607–22610
21 Wells, W. W., Xu, D. P., Yang, Y. F. and Rocque, P. A. (1990) Mammalian thioltransferase (glutaredoxin) and protein disulfide isomerase have dehydroascorbate reductase activity. J. Biol. Chem. **265**, 15361–15364
22 Maellaro, E., Del Bello, B., Sugherini, L., Santucci, A., Comporti, M. and Casini, A. F. (1994) Purification and characterization of glutathione-dependent dehydroascorbate reductase from rat liver. Biochem. J. **301**, 471–476
23 Ishikawa, T., Casini, A. F. and Nishikimi, M. (1998) Molecular cloning and functional expression of rat liver glutathione-dependent dehydroascorbate reductase. J. Biol. Chem. **273**, 28708–28712
24 Inoue, M. (1984) [Inter-organ metabolism and transport of glutathione]. Tanpakushitsu Kakusan Koso **29**, 695–707
25 Tanaka, K., Hashimoto, T., Tokumaru, S., Iguchi, H. and Kojo, S. (1997) Interactions between vitamin C and vitamin E are observed in tissues of inherently scorbutic rats. J. Nutr. **127**, 2060–2064
26 Ogiri, Y., Sun, F., Hayami, S., Fujimura, A., Yamamoto, K., Yaita, M. and Kojo, S. (2002) Very low vitamin C activity of orally administered L-dehydroascorbic acid. J. Agric. Food Chem. **50**, 227–229

27 Sugi, K., Inoue, M. and Morino, Y. (1989) Degradation of plasma bilirubin by a bilirubin oxidase derivative which has a relatively long half-life in the circulation. Biochim. Biophys. Acta **991**, 405–409
28 Iriyama, K., Yoshiura, M., Iwamoto, T. and Ozaki, Y. (1984) Simultaneous determination of uric and ascorbic acids in human serum by reversed-phase high-performance liquid chromatography with electrochemical detection. Anal. Biochem. **141**, 238–243
29 Umegaki, K., Inoue, K., Takeuchi, N. and Higuchi, M. (1994) Improved method for the analysis of ascorbic acid in plasma by high-performance liquid chromatography with electrochemical detection. J. Nutr. Sci. Vitaminol. (Tokyo) **40**, 73–79
30 Kashiba, M., Oka, J., Ichikawa, R., Kasahara, E., Inayama, T., Kageyama, A., Kageyama, H., Osaka, T., Umegaki, K., Matsumoto, A. et al. (2002) Impaired ascorbic acid metabolism in streptozotocin-induced diabetic rats. Free Radical Biol. Med. **33**, 1221–1230
31 Tietze, F. (1969) Enzymic method for quantitative determination of nanogram amounts of total and oxidized glutathione: applications to mammalian blood and other tissues. Anal. Biochem. **27**, 502–522
32 Ellman, G. L. (1959) Tissue sulfhydryl groups. Arch. Biochem. Biophys. **82**, 70–77
33 Wang, Y., Kashiba, M., Kasahara, E., Tsuchiya, M., Sato, E. F., Utsumi, K. and Inoue, M. (2001) Metabolic cooperation of ascorbic acid and glutathione in normal and vitamin C-deficient ODS rats. Physiol. Chem. Phys. Med. NMR **33**, 29–39
34 May, J. M., Qu, Z. C. and Cobb, C. E. (2004) Human erythrocyte recycling of ascorbic acid: relative contributions from the ascorbate free radical and dehydroascorbic acid. J. Biol. Chem. **279**, 14975–14982
35 Montel-Hagen, A., Kinet, S., Manel, N., Mongellaz, C., Prohaska, R., Battini, J. L., Delaunay, J., Sitbon, M. and Taylor, N. (2008) Erythrocyte Glut1 triggers dehydroascorbic acid uptake in mammals unable to synthesize vitamin C. Cell **132**, 1039–1048
36 May, J. M. (1998) Ascorbate function and metabolism in the human erythrocyte. Front. Biosci. **3**, d1–d10
37 VanDuijn, M. M., Tijssen, K., VanSteveninck, J., Van Den Broek, P. J. and Van Der Zee, J. (2000) Erythrocytes reduce extracellular ascorbate free radicals using intracellular ascorbate as an electron donor. J. Biol. Chem. **275**, 27720–27725
38 May, J. M., Qu, Z. and Cobb, C. E. (2000) Extracellular reduction of the ascorbate free radical by human erythrocytes. Biochem. Biophys. Res. Commun. **267**, 118–123
39 Su, D., May, J. M., Koury, M. J. and Asard, H. (2006) Human erythrocyte membranes contain a cytochrome b561 that may be involved in extracellular ascorbate recycling. J. Biol. Chem. **281**, 39852–39859
40 Will, J. C. and Byers, T. (1996) Does diabetes mellitus increase the requirement for vitamin C? Nutr. Rev. **54**, 193–202
41 Inoue, M. and Morino, Y. (1985) Direct evidence for the role of the membrane potential in glutathione transport by renal brush-border membranes. J. Biol. Chem. **260**, 326–331
42 Lee, J. H., Oh, C. S., Mun, G. H., Kim, J. H., Chung, Y. H., Hwang, Y. I., Shin, D. H. and Lee, W. J. (2006) Immunohistochemical localization of sodium-dependent L-ascorbic acid transporter 1 protein in rat kidney. Histochem. Cell Biol. **126**, 491–494
43 Bianchi, J. and Rose, R. C. (1985) Na^+-independent dehydro-L-ascorbic acid uptake in renal brush-border membrane vesicles. Biochim. Biophys. Acta **819**, 75–82
44 Boyer, S., Sharp, P. A., Debnam, E. S., Baldwin, S. A. and Srai, S. K. (1996) Streptozotocin diabetes and the expression of GLUT1 at the brush border and basolateral membranes of intestinal enterocytes. FEBS Lett. **396**, 218–222
45 Heilig, C. W., Brosius, 3rd, F. C. and Cunningham, C. (2006) Role for GLUT1 in diabetic glomerulosclerosis. Expert Rev. Mol. Med. **8**, 1–18
46 Linden, K. C., DeHaan, C. L., Zhang, Y., Glowacka, S., Cox, A. J., Kelly, D. J. and Rogers, S. (2006) Renal expression and localization of the facilitative glucose transporters GLUT1 and GLUT12 in animal models of hypertension and diabetic nephropathy. Am. J. Physiol. Renal Physiol. **290**, F205–F213
47 May, J. M., Cobb, C. E., Mendiratta, S., Hill, K. E. and Burk, R. F. (1998) Reduction of the ascorbyl free radical to ascorbate by thioredoxin reductase. J. Biol. Chem. **273**, 23039–23045
48 Hyun, D. H., Hunt, N. D., Emerson, S. S., Hernandez, J. O., Mattson, M. P. and de Cabo, R. (2007) Up-regulation of plasma membrane-associated redox activities in neuronal cells lacking functional mitochondria. J. Neurochem. **100**, 1364–1374
49 Samhan-Arias, A. K., Duarte, R. O., Martin-Romero, F. J., Moura, J. J. and Gutierrez-Merino, C. (2008) Reduction of ascorbate free radical by the plasma membrane of synaptic terminals from rat brain. Arch. Biochem. Biophys. **469**, 243–254

Received 19 February 2009/16 April 2009; accepted 23 April 2009
Published as BJ Immediate Publication 23 April 2009, doi:10.1042/BJ20090286

INTERNATIONAL JOURNAL OF GERIATRIC PSYCHIATRY
Int J Geriatr Psychiatry 2009; **24**: 1304–1310.
Published online 24 March 2009 in Wiley InterScience
(www.interscience.wiley.com) **DOI**: 10.1002/gps.2262

Assessment of the risk of postoperative delirium in elderly patients using E-PASS and the NEECHAM Confusion Scale

Hideyuki Hattori[1]*, Junichi Kamiya[2], Hiroshi Shimada[3], Hirotoshi Akiyama[3], Akihiro Yasui[4], Kojiro Kuroiwa[5], Koji Oda[6], Masahiko Ando[7], Takashi Kawamura[7], Atsushi Harada[8], Yuichi Kitagawa[9] and Shinji Fukata[9]

[1]*Department of Psychiatry, National Center for Geriatrics and Gerontology, 36-3 Gengo, Morioka-machi, Obu City, Aichi Prefecture, Japan*
[2]*Department of Surgery, Aichiken-Kouseiren-Toyota-Kousei Hospital, Ibohara 500-1, Jousui, Toyota city, Aichi, Japan*
[3]*Department of Gastroenterological Surgery, Yokohama City University Graduate School of Medicine, Yokohama, Japan*
[4]*Department of Surgery, Aichi-Saiseikai Hospital, Nagoya, Japan*
[5]*Department of Surgery, Tokyo Metropolitan Geriatric Hospital, 35-2 Sakaecho, Itabashi-ku, Tokyo, Japan*
[6]*Division of Surgical Oncology, Department of Surgery, Nagoya University Graduate School of Medicine, 65 Tsuruma-Cho, Showa-Ku, Nagoya, Japan*
[7]*Department of Preventive Services, Kyoto University School of Public Health, Kyoto University, Japan*
[8]*Department of Restorative Medicine, National Center for Geriatrics and Gerontology, 36-3 Gengo, Morioka-machi, Obu City, Aichi Prefecture, Japan*
[9]*Department of Surgery, National Center for Geriatrics and Gerontology, 36-3 Gengo, Morioka-machi, Obu City, Aichi Prefecture, Japan*

SUMMARY

Background The incidences of surgery-field disorders such as femur neck fracture and colorectal cancer in elderly persons have increased with the rapid aging of society. In such patients, postoperative delirium is also frequent. Patients should be generally assessed from the aspect of both physical and mental conditions in order to predict a high-delirium risk group. If so, delirium may be prevented more efficiently. In this study, we investigated whether the early detection of postoperative delirium in elderly patients is possible using a simple, useful behavior-assessing scale, the NEECHAM Confusion Scale, and a method for comprehensively evaluating elderly persons' stress related to surgery, E-PASS.

Methods The subjects were 160 patients aged more than 75 years who underwent surgery. Among them, three patients had vascular surgery-field disorders, 67 had orthopedic-field disorders, and 90 had digestive surgery-field disorders. To comprehensively evaluate surgery-related stress, E-PASS was employed. In addition, we assessed recognition, activities of daily living (ADL), and the quality of life (QOL). For delirium diagnosis and severity assessment, we used the NEECHAM Confusion Scale. The cut-off value of the NEECHAM score was established as 20 points, and patients showing values less than this after surgery were regarded as having postoperative delirium. Evaluation was performed until 10 days after surgery.

Results Postoperative delirium was noted in 54.7% of the subjects. There was a decrease in the NEECHAM score between the first and fourth postoperative days, but it gradually increased thereafter. Both uni- and multivariate analyses showed that postoperative delirium was associated with an advanced age (more than 80 years), low preoperative NEECHAM and MMSE scores, the preoperative QOL, and E-PASS. In groups showing an MMSE score of less than 25 or a preoperative NEECHAM score of less than 27, the incidence of postoperative delirium was 76%.

Conclusion The results suggest that E-PASS and the NEECHAM score facilitate assessment of the risk of postoperative delirium in elderly patients, contributing to early prevention/treatment. Copyright © 2009 John Wiley & Sons, Ltd.

KEY WORDS—elderly; delirium; E-PASS; NEECHAM

*Correspondence to: H. Hattori, Department of Psychiatry, National Center for Geriatrics and Gerontology, 36-3 Gengo, Morioka-machi, Obu City, Aichi Prefecture, Japan. E-mail: hideyuki@ncgg.go.jp

Received 19 July 2008
Accepted 9 February 2009

INTRODUCTION

Delirium is characterized by the reduction of consciousness/recognition and disturbance in the sleep/awakening rhythm. As it develops suddenly and causes various psychiatric symptoms/behavioral abnormalities, its care is difficult in most patients. In elderly patients, it is known that mental/physical stress induces delirium (Johnson, 1990). A study reported that delirium was observed in 9.6% of elderly patients who received emergency treatment (Elie *et al.*, 2000). Etiological factors for delirium in elderly patients vary. In addition to delirium related to malignant tumors or infection, its onset as an adverse reaction to drugs must be considered. However, postoperative delirium is also frequent; it is observed in 51% of patients undergoing abdominal surgery and in 48–55% of those after surgery for femur neck fracture (Olin *et al.*, 2005; Santana Santos *et al.*, 2005; Golderberg *et al.*, 2006). In Japan, the incidences of surgery-field disorders such as femur neck fracture and colorectal cancer in elderly persons have increased with the rapid aging of society (Committee for Osteoporosis Treatment, 2004; Isobe *et al.*, 2007). Internationally, an advanced age is not considered to be a contraindication for surgery. Surgery has also been positively performed in patients aged more than 90 years (nonagenarian) (Blansfield *et al.*, 2004). However, there are many risks related to the postoperative management of elderly patients. Postoperative delirium also makes postoperative management difficult.

When delirium develops, intensive drug therapy is required, causing adverse reactions; therefore, treatment is difficult in many elderly patients. A study indicated that this contributed to an increase in the mortality rate (McCusker *et al.*, 2002), cognitive hypofunction, and prolongation of the admission period (McCusker *et al.*, 2003). Delirium prevention is needed. However, its early detection is difficult in many cases. If a high-risk group can be predicted, delirium may be prevented more efficiently. Concerning the risk of postoperative delirium in elderly patients, previous studies have reported various factors. According to a systematic review conducted by Dasgupta *et al.*, risk factors for postoperative delirium include age, gender, cognitive dysfunction, mental state, previous treatment with antipsychotic agents, complications, an increase in the serum blood urea nitrogen (BUN) level, admission to a nursing home, and the reduction of activities of daily living (ADL) (Dasgupta and Dumbrell, 2006). Another study reported that risk factors for femur neck fracture, which is frequent in elderly persons, included age and cognitive hypofunction (Bitsch *et al.*, 2004). The level of risk is wide-ranging, and it is difficult to evaluate the risk before and after surgery, when various physical situations must be controlled. Therefore, a quantitative index that facilitates the pre-/intraoperative assessment of patients' physical/mental risks and evaluation of the presence or absence and severity of postoperative delirium should be employed.

In this study, we investigated whether a high-risk group in which postoperative delirium frequently develops can be selected among elderly persons using the NEECHAM Confusion Scale, which facilitates the simple, accurate diagnosis/evaluation of patients' delirium conditions, and the Estimation of Physiologic Ability and Surgical Stress (E-PASS), in which pre-/intraoperative risks can be comprehensively evaluated.

SUBJECTS AND METHODS

The subjects were 160 patients who underwent surgery between April 1, 2005 and March 31, 2008 in hospitals for which collaborative investigators worked. Among them, three patients were with vascular surgery-field disorders, 67 were with orthopedic-field disorders, and 90 were with digestive surgery-field disorders. The sites of hospitals in which evaluation was performed, hospital bed capacity, annual number of surgical procedures, and standard delirium management are shown in Table 1.

Table 1. Profiles of partipating hospitals

	Location	No of inpatients	No of surgery per year	Delirium protocol
National Center for Geriatrics and Gerontology	Aichi	300	620	Conventional therapy at onset
Aichi-Saiseikai Hospital	Aichi	324	201	Conventional therapy at onset
Tokyo Metropolitan Geriatric Hospital	Tokyo	887	617	Conventional therapy at onset
Yokoham a City University Graduate School of Medicine	Kanagawa	623	1093	Conventional therapy at onset

Int J Geriatr Psychiatry 2009; **24**: 1304–1310.
DOI: 10.1002/gps

REGISTRATION/EXCLUSION CRITERIA

We registered patients aged more than 75 years who were admitted to hospitals participating in this study, and for whom abdominal surgery-field, vascular surgery-field, and orthopedic-field surgical procedures were indicated. Only patients from whom written informed consent could be obtained 3–5 days before surgery were enrolled. We excluded those who underwent emergency surgery. In addition, those with severe dementia and those in whom psychiatric symptoms/behavioral abnormalities before surgery required treatment were excluded. For evaluation, written informed consent regarding the purpose of this study and the protection of personal information was obtained from the subjects and their families. Prior to this study, the protocol was approved by the ethics review board of each hospital.

EVALUATION ITEMS

In this study, the E-PASS items were examined to assess surgery-related physical risks. E-PASS was calculated as described in Appendix. As preoperative ADL and the quality of life (QOL) in elderly patients undergoing surgery may influence their postoperative mental state, we also evaluated these two parameters. For ADL evaluation, we employed the Barthel Index. To evaluate the QOL, we used SF-8 and EQ-5D, which can be simply conducted via an inquiry. Furthermore, the patient's preoperative condition can be accurately assessed by classifying the QOL into inferior items such as the physical component summary (PCS) and mental component summary (MCS) and expressing them as numerical data (Fukuhara and Suzukamo, 2004; Brooks R with the EuroQol Group, 1996). In addition, we evaluated age, gender, cognitive function (Mini-Mental State Examination (MMSE)), preoperative urinary incontinence, the number of catheters inserted after surgery, and agents (antipsychotic agents, hypotensive agents, and others). We also assessed anti-Parkinson agents, which may cause hallucination. The preoperative baseline data on inferior mental items in all patients are shown in Tables 2 and 3. Surgeons evaluated risk factors and the presence or absence of delirium 3–5 days before surgery, as well as surgery-related risk factors after surgery. Establishing the cut-off value of the NEECHAM score as 20 points according to the literature, patients showing values less than this after surgery were regarded as having postoperative delirium (Neelon *et al.*, 1996). In our subjects, prophylactic therapy with antipsychotic agents was not performed.

Table 2. Baseline data

Demographic analysis	Value
Surgery	
Gastrointestinal	90 (56.2%)
Orthopedics	67 (41.8%)
Vascular	3 (2.0%)
Anesthesia	
General	132 (82.5%)
Lumbar	27 (16.8%)
Local	1 (0.7%)

$N = 160$: Male/Female ratio = 68:92; Age (SD) = 81.1 (6.3)

When marked symptoms of delirium made management difficult, standard delirium treatment was administered. Nurses evaluated patients' 24-h conditions using the NEECHAM Confusion Scale every day until 10 days after surgery.

We statistically examined the association with the above risk factors. For statistical analysis, we performed univariate and multivariate analyses. For the former analysis, we prepared a univariate division table involving the NEECHAM score and risk factors, and employed the logistic regression for continuous variables and the chi-square test for categorical variables. For the latter analysis, we used a logistic model in which the presence or absence of postoperative delirium was regarded as a result variable. We regarded six factors, age, gender, department, anesthesia, MMSE, and the preoperative NEECHAM

Table 3. Baseline data

Preoperative status and surgical stress	Average	SD
MMSE	22.2	8.0
NEECHAM score	26.1	5.5
Activity of daily living (Barthel Index)	76.6	33.1
QOL (PCS)	41.3	13.3
QOL (MCS)	45.6	9.8
Hemoglobin (g/dL)	12.1	2.0
Hematocrit (%)	33.6	5.9
Albumin (g/dL)	3.6	0.5
Na mEq/L	140.2	4.1
K mEq/L	4.1	0.4
Cl (mEq/L)	103.8	4.1
BUN (mg/dL)	17.1	7.7
Creatinin (mg/dL)	0.7	0.3
Glucose (mg/dL)	120.9	48.6
Creactive protein (mg/dL)	1.7	2.9
Electrocardiogram QTc (ms)	425.7	37.1
Ultrasonic cardiogram Ejection Fraction (%)	68.1	7.7
Preoperative SpO_2 (%)	96.1	2.7
Number of catheters (post-operation)	4.2	2.0
PRS	0.58	0.26
Surgical stress score (SSS)	0.15	0.53
CRS	0.36	0.54